J Exp Biol Advance Online Articles. First posted online on 8 March 2017 as doi:10.1242/jeb.155416
Access the most recent version at http://jeb.biologists.org/lookup/doi/10.1242/jeb.155416

Inverse dynamic modelling of jumping in the red-legged running frog *Kassina maculata*

Laura B. Porro[1,*]

Amber J. Collings[1]

Enrico A. Eberhard[1]

Kyle P. Chadwick[2]

Christopher T. Richards[1]

[1]Structure and Motion Laboratory, Department of Comparative Biomedical Sciences, Hawkshead Lane, Hatfield, AL9 7TA, United Kingdom

[2]Children's Hospital Los Angeles, University of Southern California, 4650 Sunset Boulevard, Los Angeles, CA, 90027, United States of America

*Corresponding author

E: lporro@rvc.ac.uk

Key words: locomotion, biomechanics, joint angles, force plate, inverse dynamic analysis

Journal of Experimental Biology • Advance article

Summary statement

Experimental data and inverse dynamic modelling demonstrate how forward thrust and elevation are produced in the frog hind limb, allowing frogs to jump at a wide range of angles.

Abstract

Although the red-legged running frog *Kassina maculata* is secondarily a walker/runner, it retains the capacity for multiple locomotor modes, including jumping at a wide range of angles (nearly 70°). Using simultaneous hind limb kinematics and single-foot ground reaction forces, we performed inverse dynamics analyses to calculate moment arms and torques about the hind limb joints during jumping at different angles in *K. maculata.* We show that forward thrust is generated primarily at the hip and ankle, while body elevation is primarily driven by the ankle. Steeper jumps are achieved by increased thrust at the hip and ankle and greater downward rotation of the distal limb segments. Due to its proximity to the GRF vector, knee posture appears to be important in controlling torque directions about this joint and, potentially, torque magnitudes at more distal joints. Other factors correlated with higher jump angles include increased body angle in the preparatory phase, faster joint openings and increased joint excursion, higher ventrally-directed force, and greater acceleration and velocity. Finally, we demonstrate that jumping performance in *K. maculata* does not appear to be compromised by presumed adaptation to walking/running. Our results provide new insights into how frogs engage in a wide range of locomotor behaviours and the multi-functionality of anuran limbs.

Introduction

Animals jump to move through their environment, escape predators and capture prey (Alexander, 1995; Biewener, 2003). Jumping is the dominant mode of terrestrial locomotion in anurans (Emerson, 1978), involving explosive movement from a stationary, crouched posture and potentially utilizing elastic pre-loading of tendons (Peplowski and Marsh, 1997; Roberts and Marsh, 2003; Astley and Roberts, 2014). Anuran jumping has been studied using a variety of techniques, nearly all of which have focused on taxa thought to be specialized hoppers and jumpers (Calow and Alexander, 1973; Kamel et al. 1996; Lutz and Rome, 1996b; Gillis and Biewener, 2000; Wilson et al. 2000; Kargo et al. 2002; Azizi and Roberts, 2010; Astley and Roberts, 2011). Adaptation for jumping is thought to be reflected in anuran skeletal morphology. Compared to salamanders, anurans feature elongated hind limbs, tibiofibular fusion, elongated ilia, fusion of the caudal vertebrae into a urostyle, reduction in the number of presacral vertebrae and mobility at the sacroiliac and sacro-urostylic joints (Alexander, 1995; Jenkins and Shubin, 1998; Reilly and Jorgensen, 2011). However, anurans engage in locomotor behaviours other than jumping, and skeletal morphology in some groups may be adapted for these modes (Emerson, 1979, 1982; Reilly and Jorgensen, 2011). For example, variations in relative limb lengths have been associated with differential jumping ability (Zug, 1972) and both Emerson (1979, 1982) and Reilly and Jorgensen (2011) associated variations in pelvic musculoskeletal morphology with diverse locomotor behaviours. Reilly and Jorgensen (2011) even suggested walking – not jumping – as the basal anuran locomotor mode.

Kassina maculata Duméril 1853 (red-legged running frog) is a secondary walker – despite belonging to the arboreal Hyperoliidae, *K. maculata* uses a walking/running gait as its primary locomotor mode (Ahn et al. 2004; Danos and Azizi, 2015). However, *K. maculata* also climbs, burrows, swims and jumps (Loveridge, 1976; McAllister and Channing, 1983). We recorded 3D limb and body kinematics in *K. maculata* while simultaneously collecting single-foot forces exerted during jumping at a wide range of angles. These data were used to carry out inverse dynamics analysis and calculate the external moments acting about the hind limb joints during jumping in a walking (as opposed to jumping) frog taxon for the first time. We hypothesize that, based on kinematics analysis (Richards et al. *submitted*), forward thrust is produced by hip, knee and ankle extension whereas elevation is produced at the ankle and knee; it is at these joints that we expect fine-tuning of jump angle to be achieved. Specifically, steeper jump angles require higher ankle and knee torques to drive downward rotation of the distal limb elements to elevate the body.

MATERIALS AND METHODS

Animal husbandry

Data were collected from four adult *K. maculata* with mean body mass of 28.4 g ± 3.7 g and a mean snout-vent length (SVL) of 60.0 mm ± 1.2 mm (see supplementary material Table S1 for full information) obtained from commercial suppliers (AmeyZoo, Bovingdon, UK) and housed in the Biological Services Unit at the Royal Veterinary College, Hatfield, UK. Animals were housed in 45x45x45 cm terrariums (Exo Terra, Montreal, Canada) in a temperature-controlled room set at 19 - 26°C and 25 – 60% relative humidity on a 12 h:12 hour reversed light:dark cycle. Terrariums contained vegetation, hiding places, a small pool and a substrate of coco fibre, and were misted twice daily. Frogs were fed crickets, waxworms and bloodworms three times per week; once a week, crickets were dusted with mineral powder. All husbandry and experimental procedures were in accordance with UK Home Office regulations (Licence 70/8242) and Royal Veterinary College Ethics and Welfare Committee.

Data collection

External skin markers were made by cutting white plastic circles using a screw punch (Nonaka Mfg. Co. Ltd., Japan) with a 5 mm hollow point drill bit; these circles were painted on one side with a black marker. Seven markers were applied to anatomical landmarks on the body and the left hind limb using cyanoacrylate adhesive (Fig. 1A). Forces exerted during jumping were recorded using a Nano17 force/torque transducer (ATI Industrial Automation, Apex, NC, USA) mounted in a purpose-built trackway. To record single-foot forces, a small stiff aluminium plate (flush with the trackway surface) was rigidly fixed to the load cell providing sufficient area for foot contact. Force data during jumping were acquired at 2000 Hz with acquisition to PC (NI-6289) controlled by a custom-written LabVIEW (National Instruments, Austin, TX, USA) script. Frogs were simultaneously filmed at 250 frames s^{-1} at a 1/1500s shutter speed using two high-speed Photron FASTCAM cameras (Photron Ltd, San Diego, USA) positioned dorsal and lateral to the force plate; an angled mirror placed opposite the lateral camera at 60° from the horizontal was used to obtain a third view. A custom-built 49 point calibration object was used to calibrate the three views. Video data were acquired using the Photron FASTCAM Viewer and synchronized with force data using a post-trigger. Both the cameras and force transducer used a right-handed global reference frame in which the X-axis (mediolateral) pointed right, the Y-axis (fore-aft) pointed forward and the Z-axis (dorsoventral) pointed up (Fig. 1A). Frogs were positioned with the marked left hind leg resting on the force plate (to obtain single-foot forces) and facing the lateral camera, and were encouraged to jump forwards (positive Y) to a dark box by sudden movements or gentle tapping of the unmarked hind foot. A range of jump angles were elicited by varying the height of the box. Trials were conducted at 22.5 °C. After experiments animals were weighed and measured, and markers were gently removed.

Data extraction and processing

Kinematic data from the three views were calibrated and markers digitized to XYZ coordinates using open source script (Hedrick, 2008) in MATLAB (MathWorks, Natick, USA). An eighth point representing the estimated center of pressure (COP) of the marked foot was digitized. It was assumed that the Y (fore-aft) position of the COP was the most posterior point of the foot contacting the substrate in each frame and its X (mediolateral) location was along the foot midline.

Force and kinematic data were processed and analysed using custom-written scripts in Mathematica 10.0 (Wolfram Research, Champaign, USA). Strain output from the transducer was converted to XYZ components of the force exerted by the frog using a factory-supplied calibration and zeroed at take-off. Both XYZ coordinate and force data were smoothed by a 2^{nd} order reverse Butterworth low-pass filter using a cut off frequency of 25 Hz; *data were not filtered further.* Although only non-turning jumps were included in our analyses (see below), frogs rarely jumped exactly parallel to the Y axis. An axis defined by the cranial and vent markers (**B**) was used to calculate yaw angle ($\boldsymbol{\alpha}$) of the frog relative to the Y axis (**Y**), defined as [0,1,0] (Eqn 1).

$$\boldsymbol{\alpha} = \cos^{-1}\frac{\mathbf{B}\cdot\mathbf{Y}}{||\mathbf{B}||\cdot||\mathbf{Y}||}$$

(1).

in which . denotes the dot product. The calculated yaw angles were cancelled via a rotation matrix (**R**) about the Z axis (Eqn 2).

$$\mathbf{R} = \begin{bmatrix} \cos(\alpha) & -\sin(\alpha) & 0 \\ \sin(\alpha) & \cos(\alpha) & 0 \\ 0 & 0 & 1 \end{bmatrix}$$

(2).

Thus, for each frame, the 8 (markers) x 3 (XYZ coordinates) kinematic data matrix (**M**) was rotated about the Z axis so that the body axis of the frog is aligned with the Y axis throughout the jump (**M'**) (Eqn 3).

$$\mathbf{M}' = (\mathbf{R}^{\mathbf{T}}\cdot\mathbf{M}^{\mathbf{T}})^{\mathbf{T}}$$

(3).

in which **T** is the matrix transpose. This rotation matrix was also applied to the XYZ force components. Lastly, force data were down-sampled to synchronize with the kinematic data.

Force plate measurements were used to quantify **maximum vertical**, **fore-aft** and **mediolateral forces**, as well as **maximum resultant force** (both absolute and relative to body mass) and the times at which they occurred, which are presented in Table 1 and supplementary material Table S2, and in Fig. 2. Kinematic data were used to quantify the magnitude and timing of **maximum velocity** – absolute and relative to SVL – and **maximum acceleration** measured at the hip marker, which is closest to the frog's center of mass (COM). **Take-off angle** was defined as the YZ angle of the velocity vector (of the hip marker) relative to the Y axis. Our video setup did not capture the animals landing; thus, **jump distance** (**D**) was modelled using the following ballistic Eqns 4 and 5. Horizontal and vertical distance travelled through time were calculated:

$$\mathbf{D_Y} = \mathbf{V_Y} * \boldsymbol{t}$$

(4).

$$\mathbf{D_Z} = \mathbf{V_Z} * \boldsymbol{t} - \mathbf{0.5} * \boldsymbol{g} * \boldsymbol{t}^{\mathbf{2}} + \mathbf{H_{COM}}$$

(5).

in which $\boldsymbol{t}$ is time after take-off, $\mathbf{D_Y}$ is horizontal displacement, $\mathbf{D_Z}$ is vertical displacement, $\mathbf{V_Y}$ is the forward (Y) velocity at take-off, $\mathbf{V_Z}$ is the vertical (Z) velocity at take-off, $\boldsymbol{g}$ is acceleration due to gravity (9.8 ms^{-2}) and $\mathbf{H_{COM}}$ is the height of the COM at take-off. We calculated total flight time by solving for $\mathbf{D_Z}$ crossing zero – representing impact – and used this to solve for horizontal distance travelled. Kinematic performance metrics are presented in Table 1 and supplementary material Table S2.

Kinematic markers were used as a proxies for joint centers of rotation and endpoints of limb segments. Instantaneous 3D axes of rotation ($\mathbf{J_{Axis}}$) were determined for the ankle, knee, hip and sacroiliac joints using the vectors defined by the joint marker and endpoint of the proximal segment ($\mathbf{V_{Prox}}$), and by the joint marker and endpoint of the distal segment ($\mathbf{V_{Dist}}$) in Eqn 6:

$$\mathbf{J_{Axis}} = \left(\cos^{-1}\frac{\mathbf{V_{Prox}} \cdot \mathbf{V_{Dist}}}{\|\mathbf{V_{Prox}}\| \cdot \|\mathbf{V_{Dist}}\|}\right) * \mathrm{Norm}\,(\mathbf{V_{Prox}} \times \mathbf{V_{Dist}}) * -1 \tag{6}$$

(6).

in which X denotes the cross-product. The norm of this 3D axis vector gives the **3D joint angles**. **Body angle** was defined as the YZ angle formed between the head and vent markers, and the Y-axis. Maximum, minimum and range of joint angles and **peak joint angular velocities** are presented in Table 2 and Fig. 3, and supplementary material Table S2.

Force and kinematic data were used in inverse dynamics analyses to estimate external moment arms and torques acting at the hip, knee, ankle and tarsometatarsal (TMT) joints during jumping (Table 3, Figs. 4 and 5 and supplementary material Table S2). Three-dimensional external moment arm vectors ($\mathbf{V_{MA}}$) were calculated using vectors defined by the COP and GRF ($\mathbf{V_{GRF}}$) and by the COP and joint ($\mathbf{V_{Joint}}$) in Eqn 7 (Weisstein, 2009):

$$\mathbf{V_{MA}} = \|\mathbf{V_{GRF}} \times \mathbf{V_{Joint}}\| / \|\mathbf{V_{GRF}}\|$$

(7).

The norm of $\mathbf{V_{MA}}$ gives the magnitude of the external moment arm. The XYZ components of the external torques ($\mathbf{V_{Torque}}$) at each joint in world space were calculated by Eqn 8:

$$\mathbf{V_{Torque}} = \mathbf{V_{MA}} \times \mathbf{GRF}$$

(8).

in which **GRF** is the GRF vector. The norm of $\mathbf{V_{Torque}}$ is the magnitude of the 3D external torque. The norms of the XY and XZ components give torque magnitudes about the Z and Y axes, respectively, permitting us to evaluate contributions to limb protraction/retraction (i.e., anterior/posterior rotation) versus abduction/adduction (i.e., dorsal/ventral rotation) (Fig. 5, Table 3 and supplementary material Table S2). Positive (counterclockwise) XY torques indicate that the GRF acts to retract the limb segment; positive XZ torques indicate the GRF acts to abduct the limb segment (Fig. 1B, C). Internal torques generated by the frog's muscles in either plane *must* counteract external torques. Therefore, to facilitate further discussion, we will refer to joint torques from the muscles' point-of-view: negative XY torques retract limb segments whereas positive XZ torques adduct segments (Fig. 1B, C).

In addition to being analysed in absolute time, data were normalized by percent of jump contact time for comparison and statistical analyses (Figs. 2-5 and supplementary material Figs. S4 and S5). The end of each jump (in which the last toe left ground) was defined as **take-off**. **Jump start** was defined as the onset of velocity at the hip marker (closest to the COM, see Richards et al. *submitted*). Within this interval (i.e., **jump start** to **take-off**), data was resampled to 100 points using interpolation. Performance metrics were also plotted relative to take-off angle (Fig. 3) with trials classified as low, intermediate and high jumps by separating take-off angles into quantiles: **low jumps** include take-off angles below the first quantile (*n*=13, ranging from 0 to 20 degrees); **intermediate jumps** include take-off angles between the first and third quantiles (*n*=24, from 21 to 49 degrees); **high jumps** include take-off angles above the third quantile (*n*=13, from 50 to 70 degrees).

Statistical tests

Statistical tests were performed in Mathematica. General linear models (specifically, ANCOVAs) were used to investigate the relationship between jump angle (the dependent, continuous variable), individual frog (a categorical covariate) and the following separate continuous covariate performance metrics: maximum vertical, anteroposterior and total (scaled to body weight) exerted forces; maximum velocity and acceleration; 3D joint and body angles (range and maximum); maximum 3D external moment arms; and maximum 3D, XY and XZ moments (supplementary material Table S3). We also tested for interaction effects between individuals and the covariate performance variables, and used a significance threshold of $p = 0.05$ for the regression component.

CT-scanning

One individual was scanned using micro-computed tomography (µCT) at the Cambridge Biotomography Centre (University of Cambridge, UK) on an X-Tek H 225 µCT scanner (Nikon Metrology, Tring, UK) at 65 kV and 340 µA producing 1158 TIFF images with a resolution of 0.0493 mm/voxel. Scans were processed in Avizo 8.0 (FEI, Oregon, USA) producing 3D models of the bones and soft-tissues of the left foot, tarsus, shank, thigh, and body (pelvis-abdominal-thoracic segment, head and fore limbs). The long-axis of each segment was aligned with the global Y axis and the proximal joint of each segment (vent of the body segment) directed towards the origin; the dorsal aspect of each segment was directed towards positive Z. A custom-written MATLAB script (Allen et al. 2013) was used to calculate mass, COM location and moments of inertia about all axes for each segment (the latter two measured from the proximal joint), assuming a density of 1.93 g cm^{-3} for bone and 1.056 g cm^{-3} for soft tissue (Blitz & Pellegrino, 1969) (supplementary material Table S1). Three-dimensional surfaces were used to create figures and a 3D PDF (supplementary material 3D PDF S6) using Tetra4D Reviewer (Tech Soft 3D, Oregon, USA) and Adobe Acrobat Pro X (Adobe Systems Inc., California, USA).

Sensitivity Analyses

The position of the COP was estimated to account for its movement as the foot peels off the ground during take-off. We tested the sensitivity of our results to alternate COP locations for three trials: KM04 HOP 12, KM04 HOP 09 and KM04 HOP 14 (low, intermediate and high-angle jumps, respectively). A random point between the estimated COP (most posterior point of the left foot contacting the ground) and the distal tip of the fourth toe (the last to leave the ground) was selected for each time frame; this was repeated 100 times for each trial, and torques about joints calculated and compared to those produced using our estimated COP (supplementary material Fig. S4).

To understand the impact of limb inertial properties on our inverse dynamics results, we built a skeletal model with accurate segment masses and moments of inertia (see above) and imported it into the MuJoCo (Roboti LLC, Washington, USA) physics engine to solve for internal joint torques (Todorov et al. 2012; supplementary material Fig. S5).

RESULTS

Fifty jumps were recorded from four frogs. Only the trials that met the following criteria were included in analysis: 1) the frog did not turn during the jump and hind leg extension was symmetric; 2) the frog took off fully; and 3) all external markers were visible throughout the jump.

Forces exerted during jumps

Peak total force (single foot force x 2) exerted during jumping ranged from 1.7 to 4.9 x body weight, with an average of 3 x body weight (Table 1, and supplementary material Table S2). Maximum vertical force exceeded (84% of trials) and peaked earlier than (90% of trials) maximum horizontal force (Fig. 2). Across all trials, peak mediolateral forces averaged -0.01 N, an order of magnitude lower than mean peak fore-aft forces. The frog exerts a ventrally-directed force before jumping due to its foot resting on the force plate (averaging 22% ± 6% body weight). Both anteroposterior and dorsoventral forces are negative during the jump. Mediolateral forces exhibited high variability but were generally positive early in the jump, becoming negative prior to take-off (Fig. 2A). Thus, frogs pushed downwards, posteriorly and *medially* against the substrate early in the jump, then pushed downwards, posteriorly and *laterally* against the ground late in jumping. ANCOVA testing revealed strong positive correlations ($p < 1 \times 10^{-15}$) between both higher dorsoventral and higher total exerted forces, and higher-angle jumps (supplementary material Table S3). In contrast, there was no correlation between anteroposterior force and jump angle.

Velocity, acceleration, jump angle and distance, and timings

The highest recorded velocity during jumping in *K. maculata* was 2.02 ms^{-1}, with average peak velocity across all trials of 1.36 ms^{-1} (Table 1 and supplementary material Table S2). Scaled to body length, peak velocity across all trials was 33.1 SVL s^{-1} with a mean of 22.6 SVL s^{-1}. Maximum acceleration recorded across all jumps was 79.5 ms^{-2} with an average peak of 35.6 ms^{-2}. *K. maculata* exhibited wide variation in jump angles, ranging from 0.3° to 69° with a mean jump angle of 34°. Jump distance averaged 0.19 m, with a maximum distance of 0.34 m recorded. On average, peak total force and peak acceleration occurred 60 ms before take-off, and peak velocity 10 ms before take-off (Table 1). ANCOVA revealed strong correlations ($p < 0.001$) between both increased velocities (absolute and scaled to SVL) and accelerations, and higher-angle jumps (supplementary material Table S3).

3D limb kinematics

In 49 of 50 trials, the hip, knee and ankle joints opened in a proximal to distal sequence – the hip opened first, followed by the knee and, finally, the ankle (Fig. 3). For the sole exception (KM03 HOP 09, a high jump) knee and ankle extension began simultaneously. All three joints experienced similar maximum values of extension during jumping (Table 2 and supplementary material Table S2). The sacroiliac angle increased during jumping (angle change of 6° - 29°, maximum extension of 151° - 173°) while body angle (maximum values ranging between 2° - 60°) increased early in jumping then decreased during take-off (Fig. 3). Peak and final body angle increased with increasing jump angle; additionally, initial body angle (posture) was higher with increasing jump angle (Fig. 3E). Joint angular velocities increased at more distal joints and – for the body, and the hip, knee and ankle joints – angular velocities increased with jump angle (Table 2). In contrast, peak angular velocities at the sacroiliac joint were similar at low, intermediate and high-angle jumps.

ANCOVAs demonstrated very strong positive correlations ($p < 1 \times 10^{-7}$) between knee and body angles (both range of movement and maximum extension) and jump angles (supplementary material Table S3). Additionally, there were significant positive correlations ($p < 0.05$) between range of movement and maximum extension angles at the ankle, hip and sacroiliac joints, and jump angles.

Inverse dynamics: external moment arms

Maximum 3D moment arms were longest to the hip and shortened at increasingly distal joints (Table 3 and supplementary material Table S2); however, these very long moment arms occurred briefly at take-off (Fig. 4A-D) due to rapidly changing GRF vector orientation at the end of the jump and are not representative of time-averaged external moment arm lengths.

External moment arm lengths varied during jumping (Fig. 4A-D) due to changing GRF vector orientation and postural changes. As illustrated by stick figure plots (Fig. 4E-J), the GRF vector: 1) is close but typically medial and anterior to the TMT; 2) shifts from being *lateral* to *medial* of the ankle and hip joints, resulting in a brief shortening of these moment

Journal of Experimental Biology • Advance article

arms during the jump; 3) is usually medial and posterior to the knee, but closely approaches the joint during jumping, reducing moment arm length.

ANCOVAs demonstrate that maximum moment arm length to all joints *decreased* with *increasing* jump angle (Table 3 and supplementary material Table S3)

Inverse dynamics: joint torques

External torque magnitudes are controlled by GRF magnitude and external moment arm length. External moments were higher at the ankle and hip than at the TMT and knee due to the proximity of the GRF vector to the latter joints when exerted forces were highest (Table 3 and supplementary material Table S2). This proximity also explains variable XY and XZ torque traces at the TMT and knee (Fig. 5C,E) – in which the mean trace is unreflective of most individual jumps - compared to more predictable patterns at the ankle and hip (Fig. 5A,B,D,F-H), in which the mean trace *does* meaningfully reflect the general pattern. Peak XY and XZ moments are similar at the TMT, ankle and knee; in contrast, XY torques are always higher than XZ torques at the hip (Table 3 and Fig. 5).

Torque directions are controlled by the orientation of the GRF vector and its position relative to the joint (Fig. 5). The ankle and hip exhibited strong *negative* XY torques and strong *positive* XZ torques; in contrast, the knee exhibited primarily *positive* XY torques and *negative* XZ torques (Table 3 and Fig. 5). XY torques at the TMT change direction (from positive to negative) during jumping (Fig. 5) due to the changing orientation of the GRF (Fig. 6).

Three-dimensional external torque magnitudes increased during higher-angle jumps due to higher forces being exerted and *despite* shorter moment arms (Table 3, supplementary material Table S3). ANCOVAs revealed significant correlations between increased torques and higher jump angles at all joints, however, more vertical jumps were strongly correlated ($p < 0.001$) with higher negative (extension) XY torques at the ankle and hip, and higher positive (elevation) XZ torques at the ankle.

Sensitivity analyses

Joint moments using alternate COP locations are shown in supplementary material Fig. 4. Patterns resemble those from our original trials, with results converging at take-off due to the decreasing area of the foot contacting the substrate (i.e., fewer alternate COP locations). For the TMT, ankle and hip joints, torque magnitudes are higher during sensitivity analyses than in original trials because alternate COP locations *are always anterior* to our estimated COP (the most posterior point of the foot contacting the substrate). As the GRF vector typically passes anterior to these joints, alternate COP locations increase external moment arm lengths and joint torques. Varying COP location does not substantially impact torque patterns or magnitudes at the knee, possibly because the GRF vector passes close to this joint through most of the jump. Discrepancies between original trials and sensitivity analyses increase with higher-angle jumps due to higher forces. In summary, although torque magnitudes early in the jump are affected by alternate COP locations, overall torque patterns are unchanged. Therefore, the sensitivity analysis suggests that errors in the estimated location of the COP do not influence the current findings.

Peak internal torques at the TMT, ankle and knee were an order of magnitude *less* than external torques during all jumps (supplementary material Fig. 5). Internal moments at the hip were *lower* (32 – 48%) than external moments, but the discrepancy was less than at more distal joints; this is because the bulk of the body mass is being rotated and accelerated at this joint. Average internal moments (throughout the jump) at each joint were an order of magnitude *less* than average external moments; furthermore, internal moments at the hip, knee and ankle peaked substantially later than external torques. Internal moments at all joints increased during more vertical jump angles.

DISCUSSION

We have presented 3D hind limb kinematics and force data, as well as external moment arms and torques about the hind limb joints, during jumping in *K. maculata* for the first time. We hypothesized that forward thrust for jumps is produced at the hip, knee and ankle whereas elevation is produced at the ankle and knee. Our results generally support our hypothesis; however, we also found that other factors – external moment arm lengths, postural changes in the preparatory phase, faster joint opening and increased joint extension – influenced jump angle as well.

Differential production of thrust and elevation at hind limb joints controls jump angle in *Kassina*

Our analyses demonstrate *K. maculata* jumps at angles ranging from nearly horizontal to almost 70°. The ability to jump at a range of angles may be important for *K. maculata* when moving through complex, arboreal environments, as demonstrated in tree-dwelling lizards (Toro et al. 2006). How does *K. maculata* modulate jump angle?

Different relative contributions of horizontal and vertical torques at individual hind limb joints partly explain how *K. maculata* achieves a range of jump angles. Three-dimensional torques were highest around the hip and ankle, suggesting muscles acting about these joints are primarily responsible for powering jumps. Negative XY torques at the ankle and hip and positive XY torques at the knee are consistent with muscles acting to extend these joints in the XY plane, generating *thrust* and pushing the body forward (Fig. 6). Positive XZ torques at the ankle and hip and negative XZ torques at the knee are consistent with muscles acting to extend these joints in the XZ plane, producing *elevation* and pushing the body upwards (Fig. 6). Our data demonstrate that torques resulting in forward thrust increased substantially at the hip and ankle during steeper jumps while torques producing elevation increased substantially at the ankle during steeper jumps (Table 3, supplementary material Table S3). Negative XY torques *always* exceeded positive XZ torques at the hip, regardless of jump angle, suggesting most of the work at the hip is forward thrust, as reported by Astley and Roberts (2014) in *Rana*. Our findings also agree with those of Kargo et al. (2002), which suggest horizontal take-off velocity (thrust) is most sensitive to hip extensor torques. In contrast, the ankle contributes equally to thrust and elevation; inverse kinematics (IK) analysis also predicted ankle extension drives steeper jumps, particularly early in the jump (Richards et al., *submitted*). Our findings *largely* support our hypothesis – forward thrust is produced primarily at the hip and ankle whereas elevation is produced primarily at the ankle.

Results for the knee were more complicated – both positive and negative XY and XZ torques significantly increased with jump angle (supplementary material Table S3). Again, this in line with IK analysis predicting knee extension is important in increasing take-off angles late in the jump (Richards et al. *submitted*). Increased torque magnitudes were due to higher forces; variability in torque direction was due to the volatile position of the GRF vector relative to the knee. Kargo et al. (2002) predicted that increased degrees of freedom at the knee joint allows frogs to bring the foot under the body and doubles the ankle extensor torque producing vertical acceleration of the body. Similarly, IK analysis predicted reorientation of the knee rotation axis is crucial to achieving COM elevation (Richards et al. *submitted*). Thus, fluctuations in torque direction may reflect the subtle and important role of knee positioning in modulating jump angle by permitting high elevation torques to be produced at the ankle. Alternatively (or additionally), close alignment of the GRF vector to the knee joint may increase the effective mechanical advantage of the muscles crossing this joint throughout jumping (see more below).

Lastly, as the frog pushes laterally against the substrate in the final moments before take-off, the GRF vector becomes medially-directed, resulting in XY and XZ torque directions being reversed at the hip and ankle joints during some trials (Figs. 5 and 6), potentially aiding extension of these joints during take-off.

Moment arms and kinematics influence jump angle in *Kassina*

Our data show that – in addition to differential joint torques – decreased external moment arm lengths, postural changes, faster joint opening and greater joint extension also play a role in achieving high jump angles. External moment arm length *decreased* during steeper jumps. Based on lever mechanics (Eqn 9):

$$\mathbf{EMA} = \mathbf{r}/\mathbf{R} \quad (9).$$

in which **EMA** is a muscle's "effective mechanical advantage", **r** is the muscle moment arm length (presumably unchanged during jumping in frogs; Leiber and Brown, 1992; Kargo and Rome, 2002; Astley and Roberts 2011), and **R** is the external moment arm (Biewener, 1989). Closer alignment of the limb to the GRF vector during higher-angle jumps in frogs results in a shorter **R** and increases **EMA**, thus helping the frog's muscles to counter the higher GRFs associated with steeper jumps. We also found that ankle moment arm shortens as the joint begins to extend (between time points 70 and 90, Figs. 3 and 4), leading to increased EMA. This is similar to data presented by Astley and Roberts (2014) from *Rana*, and is crucial to their proposed dynamic catch mechanism, although the decrease in moment arm in *K. maculata* is less pronounced than in *Rana.* Roberts et al. (2011) demonstrated that some frog species are more likely to use power amplification by elastic recoil than others; it is possible that, as a secondary walker, this mechanism is not as important during jumping in *K. maculata* as in *Rana.*

Postural differences also characterized steeper jumps in *K. maculata.* Higher body angles were very strongly correlated with steeper jumps; specifically, higher-angle jumps featured higher-angle starting postures, controlled by the degree of arm extension (Wang et al. 2014). Videos demonstrate that during low-angle jumps, the frog's forearm is nearly parallel to the trackway and the elbow points laterally; in contrast, the forearm is at a steep angle to the trackway and the elbow positioned under the body at the beginning of high-angle jumps. High-speed video and angular velocities (Table 2) demonstrate that, during high-angle jumps, frogs rapidly pitched their bodies backwards prior to limb extension; higher body rotational velocities during steep jumps were also observed by Richards et al. (*submitted*). Kargo et al. (2002) demonstrated using forward dynamic simulations that take-off angle was most sensitive to long-axis rotation (of the femur) at the hip; although we cannot quantify internal rotation of limb bones using our methods, tilting of the body at the hip joint may play an important role in achieving high-angle jumps in *K. maculata*.

Various force and kinematic parameters were correlated with steeper jumps. Although some low and intermediate angle jumps featured high forces, *all* high-angle jumps featured increased ventrally-directed force. Thus, our findings suggest frogs can *choose* to exert more force during shallow jumps to increase distance, but they *must* exert higher forces to jump at steep angles. The ankle, knee and hip joints opened faster during more vertical jumps, and increased jump angle was also correlated with increased range of movement and extension of these joints, particularly the knee (also see Richards et al. *submitted*). Greater extension of the knee and hip joints during more vertical jumps were also reported by Lutz and Rome (1996a). We also found significant correlation of increased extension of the sacroiliac joint during steeper jumps, supporting hypotheses of sacroiliac function by Emerson and De Jongh, 1980; but unlike the body and hind limb joints, angular velocity at this joint did not increase with steeper jump angles (see also Richards et al. *submitted*).

Thus, our data demonstrate that external moment arm lengths, preparatory posture and kinematic differences also help explain how *K. maculata* achieves a wide range of jump angles. Results from IK analysis suggest that dynamic modulation of joint rotation axes during the jump are an additional means by which frogs can control jump angle (Richards et al. *submitted*).

Kassina jumping performance is similar to other frog species

We cannot rigorously test whether morphological or behavioural adaptations for walking in some frogs compromise jumping performance using a single-species test, particularly as there is limited data available for non-walking hyperoliids. Furthermore, previous studies span a restricted range of taxonomic groups and vary in experimental methodology, reported anatomical and performance metrics, animal size, temperature and motivation. Nonetheless, we can compare our jump performance metrics from *K. maculata* to similar data collected from other anurans (Table 4).

The peak resultant exerted force (multiplied by two and scaled to body mass) for *K. maculata* was above the average of the reported range (Table 4). Peak vertical force both exceeded and occurred earlier than peak horizontal force in *K. maculata*, similar to ranids (Calow and Alexander, 1973; Nauwelaerts and Aerts, 2006; Astley and Roberts, 2014; Wang et al. 2014) but unlike hylids (Marsh and John-Alder, 1994). Maximum take-off velocities in *K. maculata* were slightly below average velocity reported in other frogs, whereas jump distance (scaled to SVL) was within the range reported for ranids but substantially lower than distances recorded in hylids (Table 4). The proximal to distal pattern of joint opening observed during jumping in *K. maculata* has been widely reported among frogs (Calow and Alexander, 1973; Peters et al. 1996; Nauwelaerts and Aerts, 2003; Astley and Roberts, 2014; Wang et al. 2014) and is thought to maximize foot-to-ground contact time, prolong acceleration (so that maximum velocity is reached as late as possible) and aid in elastic energy pre-storage (Bobbert and van Ingen Schenau, 1988; van Ingen Schenau, 1989; Wang et al. 2014). Range of movement and maximum values of extension for the ankle, knee, hip and sacroiliac joints in *K. maculata* are similar to those reported in other species (Calow and Alexander, 1973; Lutz and Rome, 1996a; Peters et al. 1996; Nauwelaerts and Aerts, 2003; Astley and Roberts, 2014). Jump angle in *K. maculata* averaged 34°, within the range reported in other frogs (Table 4) but lower than the optimal angle of 42° thought to maximize jump distance (Marsh 1994). *K. maculata* are also capable of achieving a relatively wide range of jump angles (nearly 70°) compared to those reported in other frogs (Table 4).

In terms of these performance metrics and limited comparative data from other frogs, *K. maculata* appears to be an average jumper. Our results suggest that presumed anatomical/behavioural adaptations for walking in *K. maculata* do not affect jumping performance (but see Astley [2016]), echoing studies that demonstrate limited evidence for a performance trade-off between jumping and swimming (Emerson and De Jongh, 1980; Peters et al. 1996; Nauwelaerts et al., 2007; Herrel et al. 2014; Astley, 2016). It should be noted, however, that *K. maculata* is not morphologically specialized for walking to the degree found in other taxa (some microhylids, brevicepitines or hemisotids); thus, it is unknown how adaptation to walking may affect jumping performance more generally among frogs.

Conclusions

The results presented here document force and joint kinematics during jumping in *K. maculata*, as well as results from inverse dynamics analysis of the hind limb. We show that forward thrust is generated primarily at the hip and ankle, while increased elevation (permitting steeper jumps) is generated primarily at the ankle. Additionally, postural changes – including body angle in the preparatory phase and positioning of the knee – as well as decreased external moment arm length, faster joint opening and increased joint extension allow higher-angle jumps in this taxon. Furthermore, our data suggest jumping performance in *K. maculata* is not compromised by secondary adaptation to walking and running. Finally, we conducted sensitivity analyses that demonstrate: 1) alternate COP locations during take-off result in increased torque magnitudes early in the jump, but do not impact overall patterns of joint torques; and 2) peak internal torques are an order of magnitude lower than external torques at distal hind limb joints, and can be considered negligible. Internal torque magnitudes at the hip are 32 – 48% external torque magnitudes.

One limitation of our methods is the inability to visualize movements of internal structures. Previous studies (Kargo et al. 2002) have suggested the importance of long-axis rotations of hind limb bones during jumping; in contrast, Astley and Roberts (2014) found that such movements were minimal. Investigating such movements and their impact await future experiments using X-ray reconstruction of moving morphology (XROMM).

Postural changes (tilting of the body due to extension of the arms that causes rotation of the pelvis relative to the femur, and knee positioning) appear to be a major control on jump angle in *K. maculata.* Many of the major muscles that power jumping originate on the lateral aspect of the ilium and insert at or distal to the knee (Přikyl et al. 2009); thus, variations in starting posture at different jump angles would change the moment arms and, potentially, action of these muscles. Indeed, Kargo and Rome (2002) demonstrated that frog hind limb muscles have different functions depending on task and limb configuration. Future XROMM experiments and musculoskeletal modelling will allow us to explore internal rotations of the limb segments during jumping and permit detailed models of muscle function in jumping frogs, including how morphological changes during the evolution of frogs may have impacted locomotor evolution. Ultimately, work from both living and fossil anurans can be used to understand the origin of frog musculoskeletal anatomy and locomotor behaviour, and whether frog limbs were indeed built for jumping, walking or multi-functionality, with the ability to adapt to varying movements and terrains.

Acknowledgements

Alastair Wallis (RVC) cared for research animals. Steve Amos, Emily Sparkes and Timothy West (RVC) assisted with obtaining software, equipment and experimental set up. Special thanks to Vivian Allen (RVC) for his help determining segment moment of inertia. Robert Asher, Matthew Mason and Colin Shaw (University of Cambridge) provided CT-scanning time. Technical support for Avizo provided by Alejandra Sánchez-Eróstegui and Jean Luc-Garnier (FEI Visualization Sciences Group).

Competing interests

The authors declare no competing interests.

Author contributions

L.B.P., A.J.C. and C.T.R. designed the research. E.A.E. and L.B.P. constructed the experimental setup. K.P.C. built the original force plate. C.T.R. and L.B.P. wrote the LabVIEW script to collect force data. All authors collected *in vivo* experimental data. L.B.P. carried out CT-scanning and processed CT data. L.B.P. and C.T.R. wrote Mathematica scripts for data processing. L.B.P. carried out inverse dynamics analyses. C.T.R. developed code to calculate internal torques. L.B.P. drafted the manuscript. All authors read and commented on the manuscript.

Funding

Funding was provided by an European Research Council Starting Grant to C.T.R. (PIPA, Paleo-robotics and the innovations of propulsion in amphibians). Funding for K.P.C was provided by the Leverhulme Trust.

Data availability

Custom *Mathematica* scripts and original CT data used in this study can be obtained by contacting the corresponding author. All other data included as supplementary files.

References

Ahn, A., Furrow, E. and Biewener, A. (2004). Walking and running in the red-legged running frog, *Kassina maculata. J. Exp. Biol.* **207,** 399-410.

Alexander, R Mc. (1995). Leg design and jumping technique for humans, other vertebrates and insects. *Phil. Trans. R. Soc. Lond. B.* **347,** 235-248.

Allen, V., Bates, K., Li, Z. and Hutchinson, J. (2013). Linking the evolution of body shape and locomotor biomechanics in bird-line archosaurs. *Nature* **497,** 104-107.

Astley, H. (2016). The diversity and evolution of locomotor muscle properties in anurans. *J. Exp. Biol.* **219,** 3163-3173.

Astley, H. and Roberts, T. (2011). Evidence for a vertebrate catapult: elastic energy storage in the plantaris tendon during frog jumping. *Biol. Lett.* **8,** 386-389.

Astley, H. and Roberts, T. (2014). The mechanics of elastic loading and recoil in anuran jumping. *J. Exp. Biol.* **217,** 4372-4378.

Astley, H., Abbott, E., Azizi, E., Marsh, R. and Roberts, T. (2013). Chasing maximal performance: a cautionary tale from the celebrated jumping frogs of Calaveras County. *J. Exp. Biol.* **216,** 3847-3953.

Azizi, E. and Roberts, T. (2010). Muscle performance during frog jumping: influence of elasticity on muscle operating lengths. *Proc. Biol. Soc.* **277,** 1523-1530.

Biewener, A. (1989). Scaling body support in mammals: limb posture and muscle moments. *Science* **245**, 45-48.

Biewener, A. (2003). *Animal Locomotion.* Oxford: Oxford University Press, 296pp.

Blitz, R. and Pellegrino, E. (1967) The chemical anatomy of bone. I. A comparative study of bone composition in sixteen vertebrates. *J. Bone Joint Surg. Am.* **51,** 456-466.

Bobbert, M. and van Ingen Schenau, G. (1988). Coordination in vertical jumping. *J. Biomech.* **21,** 249-262.

Calow, L. and Alexander, R. McN. (1973). A mechanical analysis of a hind limb of a frog. *J. Zool. Lond.* **171**, 292-321.

Choi, I-H. and Park, K. (1996). Variation in take-off velocity of anuran amphibians: relation to morphology, muscle contractile function and enzyme activity. *Comp. Biochem. Physiol.* **4,** 393-400.

Danos N. and Azizi, E. (2015). Passive stiffness of hindlimb muscles in anurans with distinct locomotor specializations. *Zool.* **118:** 239-247.

Delp S., Anderson F., Arnold A., Loan P., Habib A., John C., Guendelman E., and Thelen D. (2007). OpenSim: open-source software to create and analyze dynamic simulations of movement. *IEEE Trans. Bio-Medical Engin*. **54,** 1940–1950.

Emerson, S. (1978). Allometry and jumping in frogs: helping the twain to meet. *Evolution.* **32,** 551-564.

Emerson, S. (1979). The ilio-sacral articulation in frogs: form and function. *Biol. J. Linn. Soc.* **11,** 153-168.

Emerson, S. (1982). Frog postcranial morphology: identification of a functional complex. *Copeia.* **3,** 603-613.

Emerson, S. and De Jongh, H. (1980). Muscle activity at the ilio-sacral articulation of frogs. *J. of Morph.* **166,** 129-144.

Gillis, G. and Biewener, A. (2000). Hindlimb extensor muscle function during jumping and swimming in the toad (*Bufo marinus*). *J. Exp. Biol.* **203,** 3547-3563.

Hedrick, T. (2008). Software techniques for two- and three-dimensional kinematic measurements of biological and biomimetic systems. *Bioinspir. Biomim.* **3:** 034001.

Herrel A., Vasilopoulou-Kampitsi, M and Bonneaud, C. (2014). Jumping performance in the highly aquatic frog, *Xenopus tropicalis*: sex-specific relationships between morphology and performance. *PeerJ.* **2** :e661 https://doi.org/10.7717/peerj.661

Hirano, M. and Rome, L. (1981). Jumping performance of frogs (*Rana pipiens*) as a function of muscle temperature. *J. Exp. Biol.* **108,** 429-439.

Jenkins, F. and Shubin, N. (1998). *Prosalirus bitis* and the anuran caudopelvic mechanism. *J. Vert. Paleontol.* **18,** 495-510.

Kamel, L., Peters, S. and Bashor, D. (1996). Hopping and swimming in the leopard frog, *Rana pipiens:* II. A comparison of muscle activities. *J. of Morph.* **230,** 17-31.

Kargo, W. and Rome, L. (2002). Functional morphology of proximal lindlimb muscles in the frog *Rana pipiens. J. Exp. Biol.* **205,** 1987-2004.

Kargo, W., Nelson, F. and Rome, L. (2002). Jumping frogs: assessing the design of the skeletal system by anatomically realistic modelling and forward dynamics simulation. *J. Exp. Biol.* **205,** 1683-1702.

Lieber, R. and Brown, C. (1992). Sarcomere length-joint angle relationships of seven frog hindlimb muscles. *Aca Anat.* **145,** 289-295.

Loveridge, J. (1976). Strategies of water conservation in southern African frogs. *Zool. Africana.* **11**, 319–333.

Lutz, G. and Rome, L. (1994). Built for jumping: the design of the frog muscular system. *Science.* **263,** 370-372.

Lutz, G. and Rome, L. (1996a). Muscle function during jumping frogs. I. Sarcomere length change, EMG pattern, and jumping performance. *Am. J. Physiol.* **271,** C563 – C570.

Lutz, G. and Rome, L. (1996b). Muscle function during jumping frogs. II. Mechanical properties of muscle: implications for system design. *Am. J. Physiol.* **271,** C571 – C578.

Marsh, R. (1994). Jumping ability of anuram amphibians. In *Advances in Veterinary Science and Comparative Medicine: Comparative Vertebrate Exercise Physiology* (ed. J.H. Jones). New York: Academic Press, **38,** 51-111.

Marsh, R. and John-Alder, H. (1994). Jumping performance of hylid frogs measured with high-speed cine film. *J. Exp. Biol.* **188,** 131-141.

McAllister, W. and Channing, A. (1983) Comparison of toe pads of some southern African climbing frogs. *S. African J. Zool*. **18**, 110-114.

Journal of Experimental Biology • Advance article

Nauwelaerts, S. and Aerts, P. (2003). Propulsive impulse as a covarying performance measure in the comparison of the kinematics of swimming and jumping in frogs. *J. Exp. Biol.* **2-6,** 4341-4351.

Nauwelaerts, S. and Aerts, P. (2006). Take-off and landing forces in jumping frogs. *J. Exp. Biol.* **209,** 66-77.

Nauwelaerts, S., Ramsay, J. and Aerts, P. (2007). Morphological correlates of aquatic and terrestrial locomotion in a semi-aquatic frog, *Rana esculenta:* no evidence for a design conflict. *J. Anat.* **210,** 304-317.

Olson, J. and Marsh, R. (1998). Activation patterns and length changes in hindlimb muscles of the bullfrog *Rana catesbeiana* during jumping. *J. Exp. Biol.* **201,** 2763-2777.

Peplowski, M. and Marsh, R. (1997). Work and power output in the hindlimb muscles of Cuban tree frogs *Osteopilus septentrionalis* during jumping. *J. Exp. Biol.* **200,** 2861-2870.

Peters, S., Kamel, L. and Pashor, D. (1996). Hopping and swimming in the leopard frog, *Rana pipiens:* I. Step cycles and kinematics. *J. Morph.* **230,** 1-16.

Přikyl, T., Aerts, P., Havelova, P., Herrel, A. and Roček, Z. (2009). Pelvic and thigh musculature on frogs (Anura) and origin of anuram jumping locomotion. *J. Anat.* **214,** 100-139.

Reilly, S. and Jorgensen, M. (2011). The evolution of jumping in frogs: morphological evidence for the basal anuran locomotor condition and the radiation of locomotor systems in crown group anurans. *J. Morph.* **272,** 149-168.

Roberts, T. and Marsh, R. (2003). Probing the limits to muscle-powered accelerations: lessons from jumping bullfrogs. *J. Exp. Biol.* **206,** 2567-2580.

Roberts, T., Abbott, E. and Azizi, E. (2011). The weak link: do muscle properties determine locomotor performance in frogs? *Phil. Trans. R. Soc. B.* **366,** 1488-1495.

Todorov, E., Erez, T. and Tassa, Y. (2012). MuJoCo: A physics engine for model-based control. *2012 IEEE/RSJ International Conference on Intelligent Robots and Systems*. IEEE, 2012.

Toro, E., Herrel, A. and Irschick, D. (2006). Movement control strategies during jumping in a lizard (*Anolis valencienni*). *J. Biomech.* **39,** 2014-2016.

van Ingen Schenau, G. (1989). From rotation to translation: constraints on multi-joint movements and the unique action of bi-articular muscles. *Hum. Mov. Sci.* **8,** 301-337.

Wang, Z., Ji, A., Endlein, T., Samuel, D., Yao, N., Wang, Z. and Dai, Z. (2014). The role of fore- and hindlimbs during jumping in the Dybowski's frog (*Rana dybowskii*). *J. Exp. Zool.* **321A,** 324-333.

Weisstein, E. (2009). Point-Line Distance--3-Dimensional. From *MathWorld--A Wolfram Web Resource.* http://mathworld.wolfram.com/Point-LineDistance3-Dimensional.html

Wilson, R., Franklin, C. and James, R. (2000). Allometric scaling relationships pf jumping [erformance om the striped marsh frog *Limnodynastes peronei. J. Exp. Biol.* **203,** 1937-1946.

Zug, G. (1972). Anuran locomotion: structure and function, I. Preliminary observations on the relation between jumping and osteometrics of appendicular and postaxial skeleton. *Copeia.* **4,** 613-624.

Figures

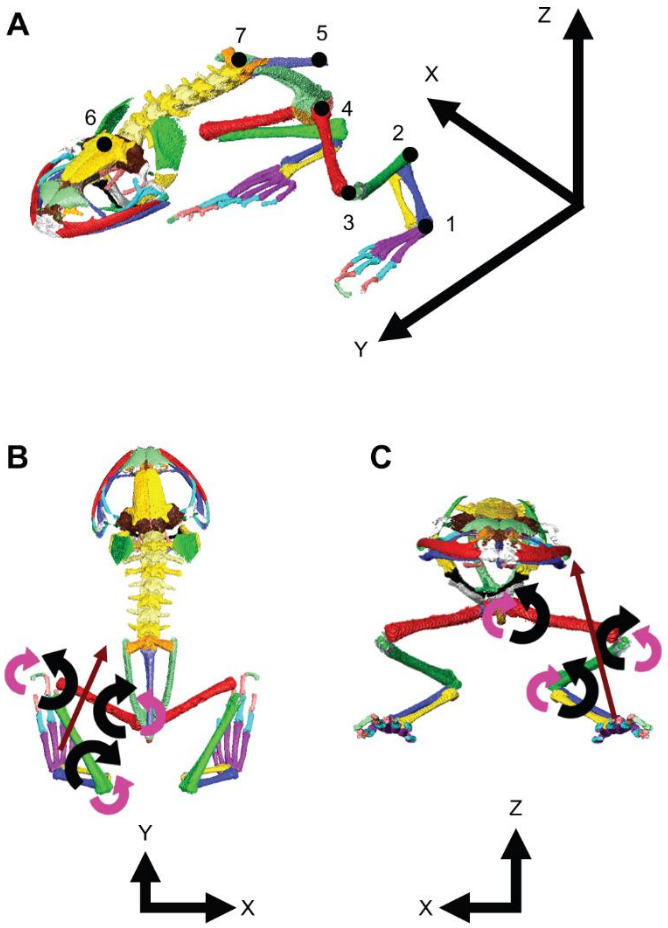

Fig. 1. Marker position, global coordinate system and torque directions. 3D skeletal model of *Kassina maculata* (from CT scans) in oblique (A), dorsal (B) and anterior (C) views. Global coordinate systems shown; in B and C, the Z and Y axes (respectively) are coming out of the page. Black dots mark the positions of the tarsometatarsal (TMT) (1), ankle (2), knee (3), hip (4), vent (5), head (6) and sacral (7) kinematic markers in A. In B and C, dark red arrows show the approximate orientation of the ground reaction force midway through a jump; curved black arrows show the directions of the external torques (generated by ground reaction force) on the ankle, knee and hip joints; curved pink arrows show the directions of the opposing muscle torques required to balance external torques.

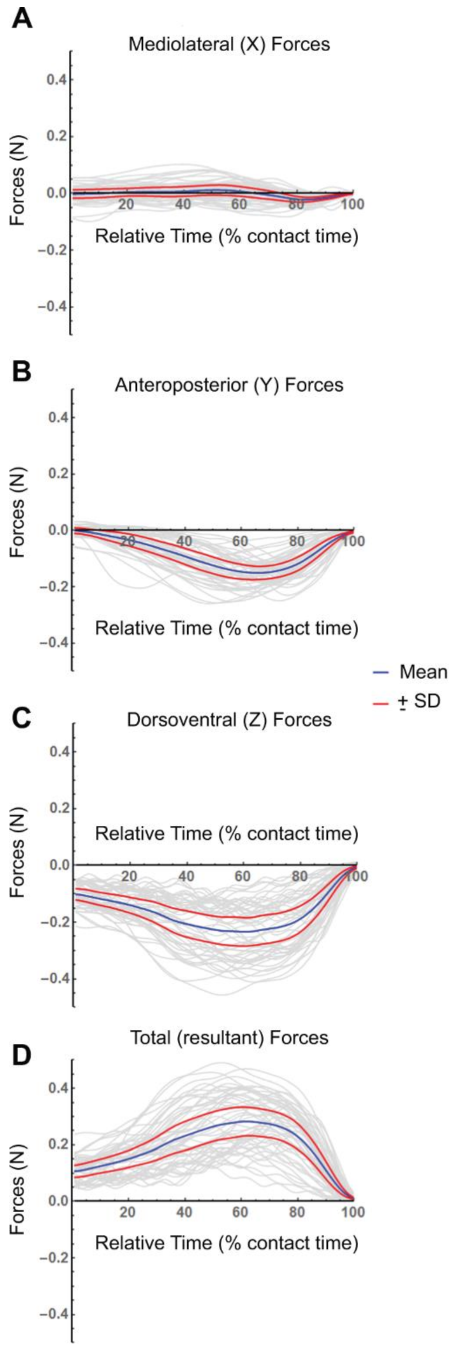

Fig. 2. Single-foot forces exerted during jumping in *Kassina maculata.* Data from 50 trials and 4 individuals are normalized and resampled to 100 time points using methods described in the text and shown to the same scale for all trials (A – D), including mediolateral (A), anteroposterior (B), dorsoventral (C) and total resultant (D) forces. Blue traces indicate mean force values; red traces indicate standard deviation; traces for individual trials are shown in gray.

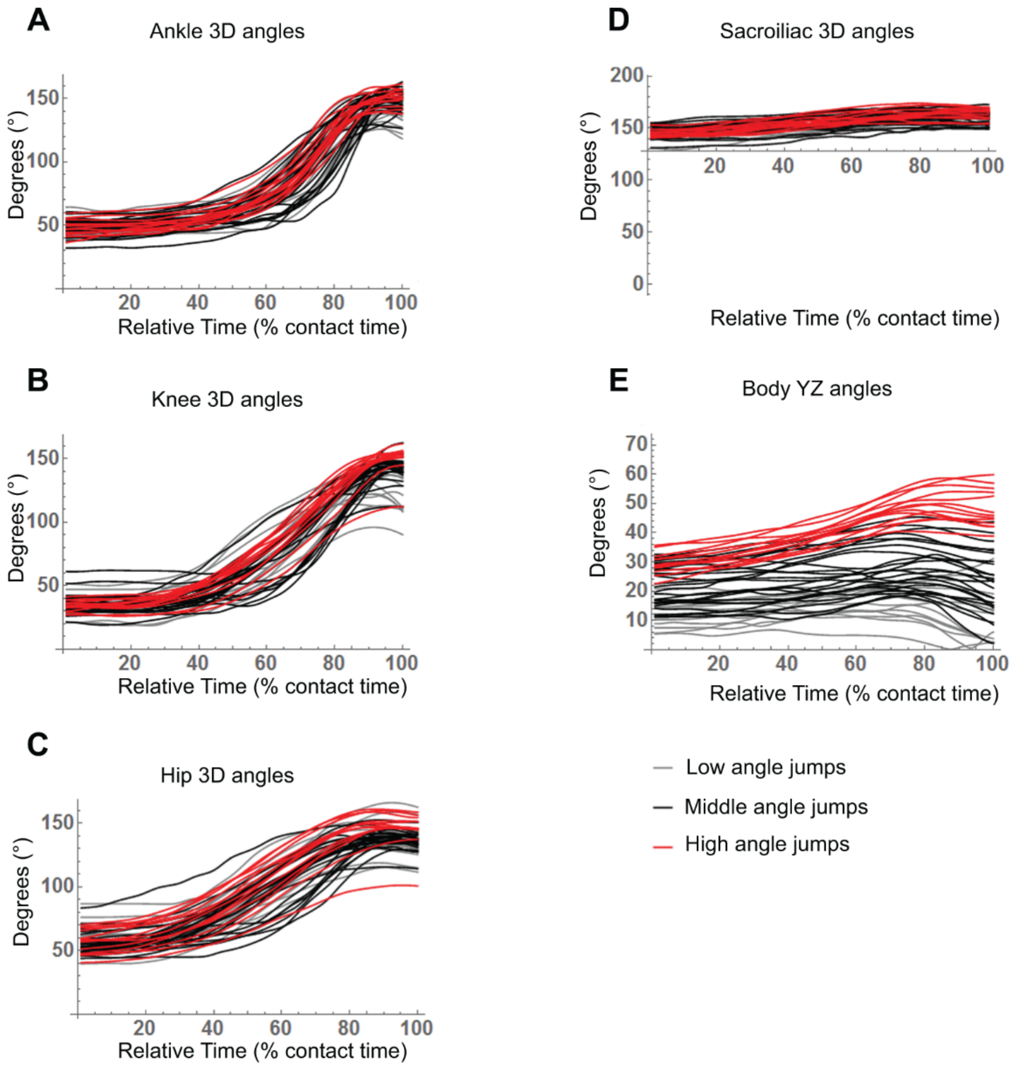

Fig. 3. Joint angles during jumping in *Kassina maculata.* Three-dimensional ankle (A), knee (B), hip (C) and sacroiliac (D) angles and YZ body angles (E). Data are normalized and resampled to 100 time points. Trials are separated by jump angle (see text): gray traces indicate low-angle jumps; black traces indicate intermediate-angle jumps; red traces indicate high-angle jumps.

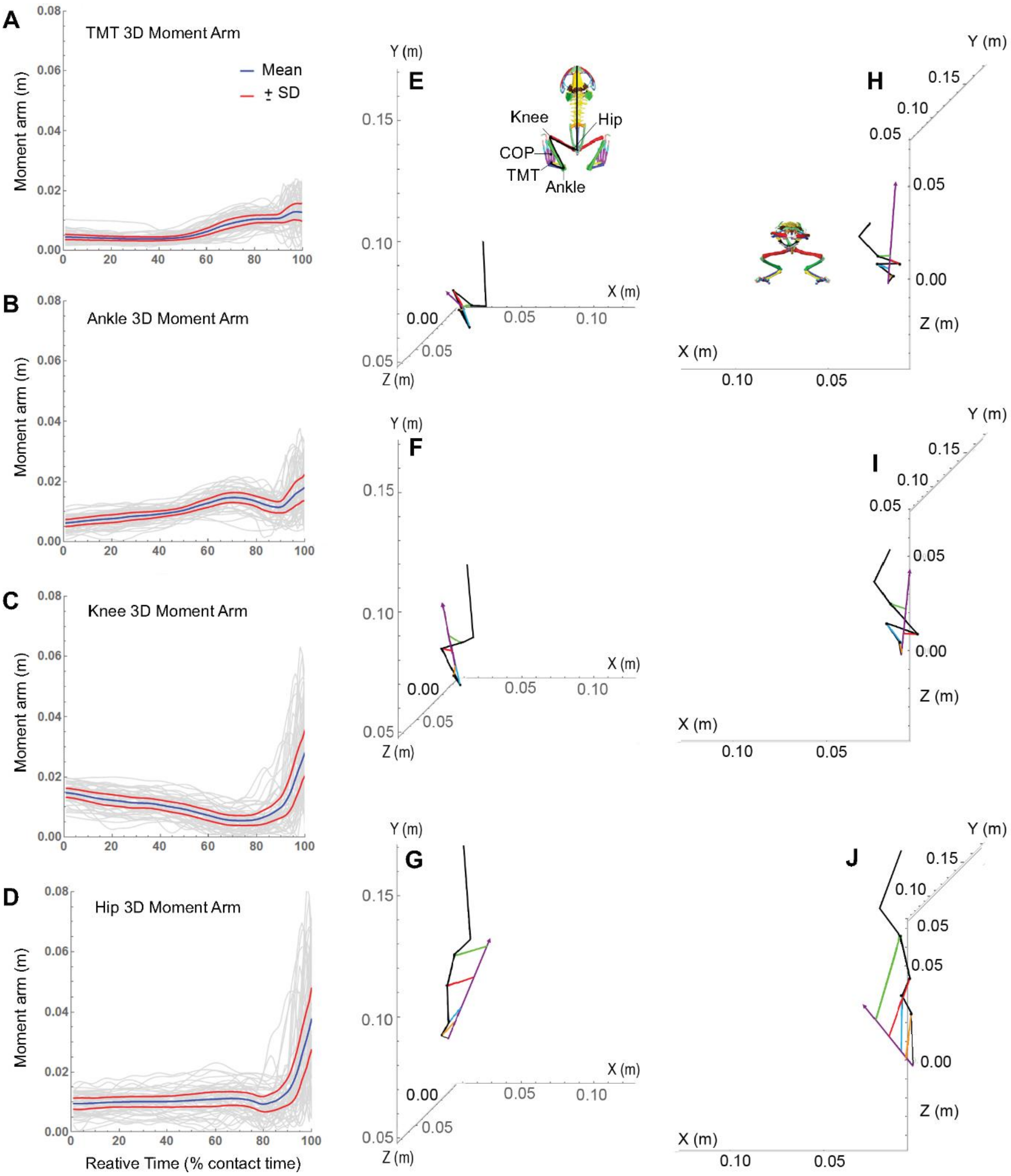

Fig. 4. External moment arms about hind limb joints during jumping in *Kassina maculata.* 3D external moment arms about the tarsometatarsal (TMT) (A), ankle (B), knee (C) and hip (D) joints; data are normalized and resampled to 100 time points and shown to the same scale. For A-D, blue traces indicate mean moment arm lengths; red traces indicate standard deviations; traces for individual trials are shown in gray. Stick figure plots (E – J) show the

Journal of Experimental Biology • Advance article

frog's body and left hind limb in dorsal (E-G) and anterior (H-J) views as segments, the GRF vector (in purple) and external moment arms from the hind limb joints during an exemplar, intermediate-angle jump (KM04 HOP 09) at 44 ms (E, H), 184 ms (F, I) and 240 ms (G, J) into the jump.

Journal of Experimental Biology • Advance article

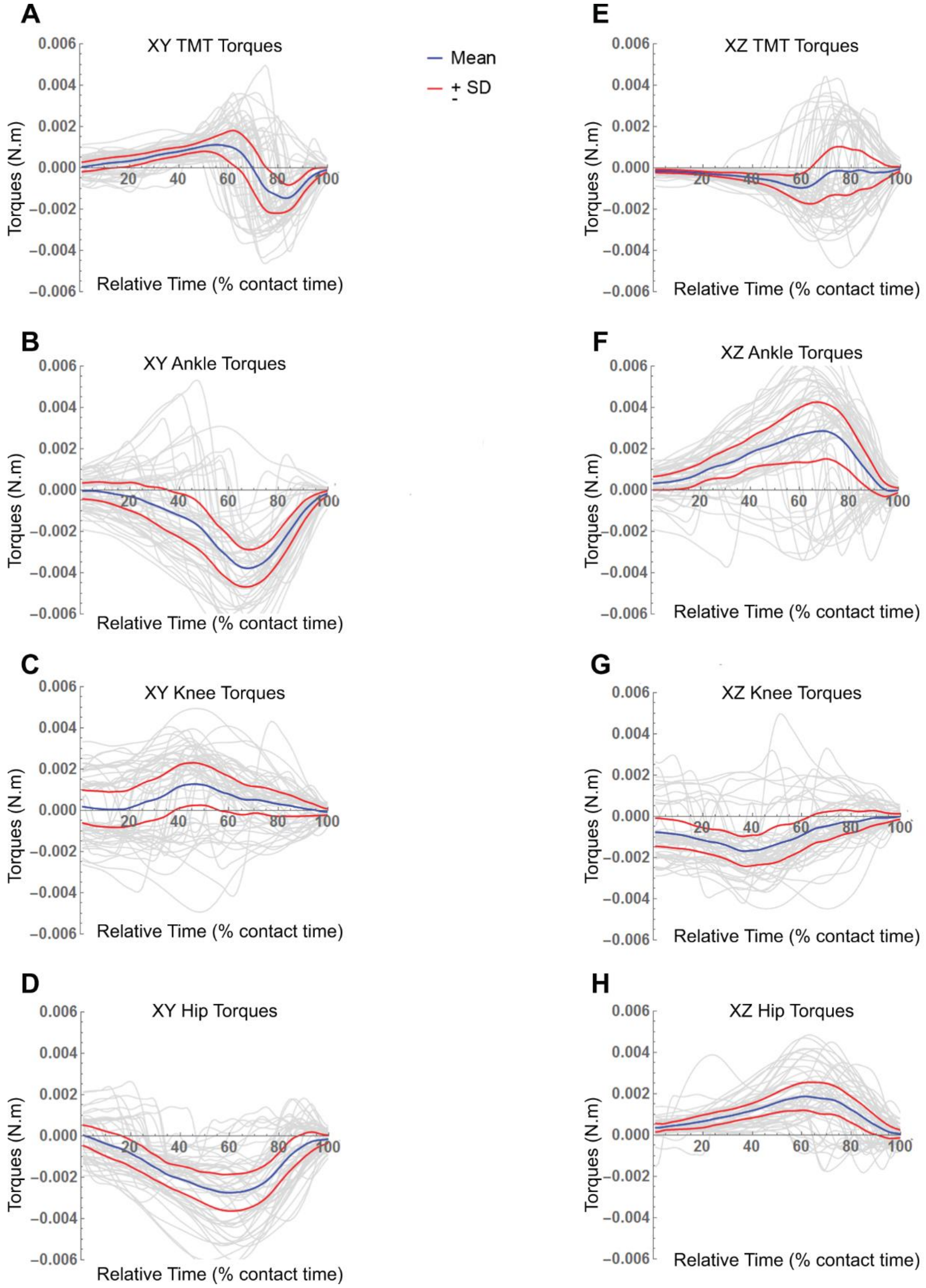

Fig. 5. External torques about the hind limb joints during jumping in *Kassina maculata*. Torques about the tarsometatarsal (TMT) (A, E), ankle (B, F), knee (C, G) and hip (D, H) joints for in the XY (horizontal plane, A-D) and XZ (transverse vertical plane, E-H) planes. For XY torques, negative values indicate retraction of the segment relative to the body

(from the muscle's point-of-view). For XZ torques, positive values indicate adduction of the segment relative to the body. Data are normalized and resampled to 100 time points and are shown to the same scale. Blue traces indicate mean values; red traces indicate standard deviations; traces for individual trials are shown in gray.

Journal of Experimental Biology • Advance article

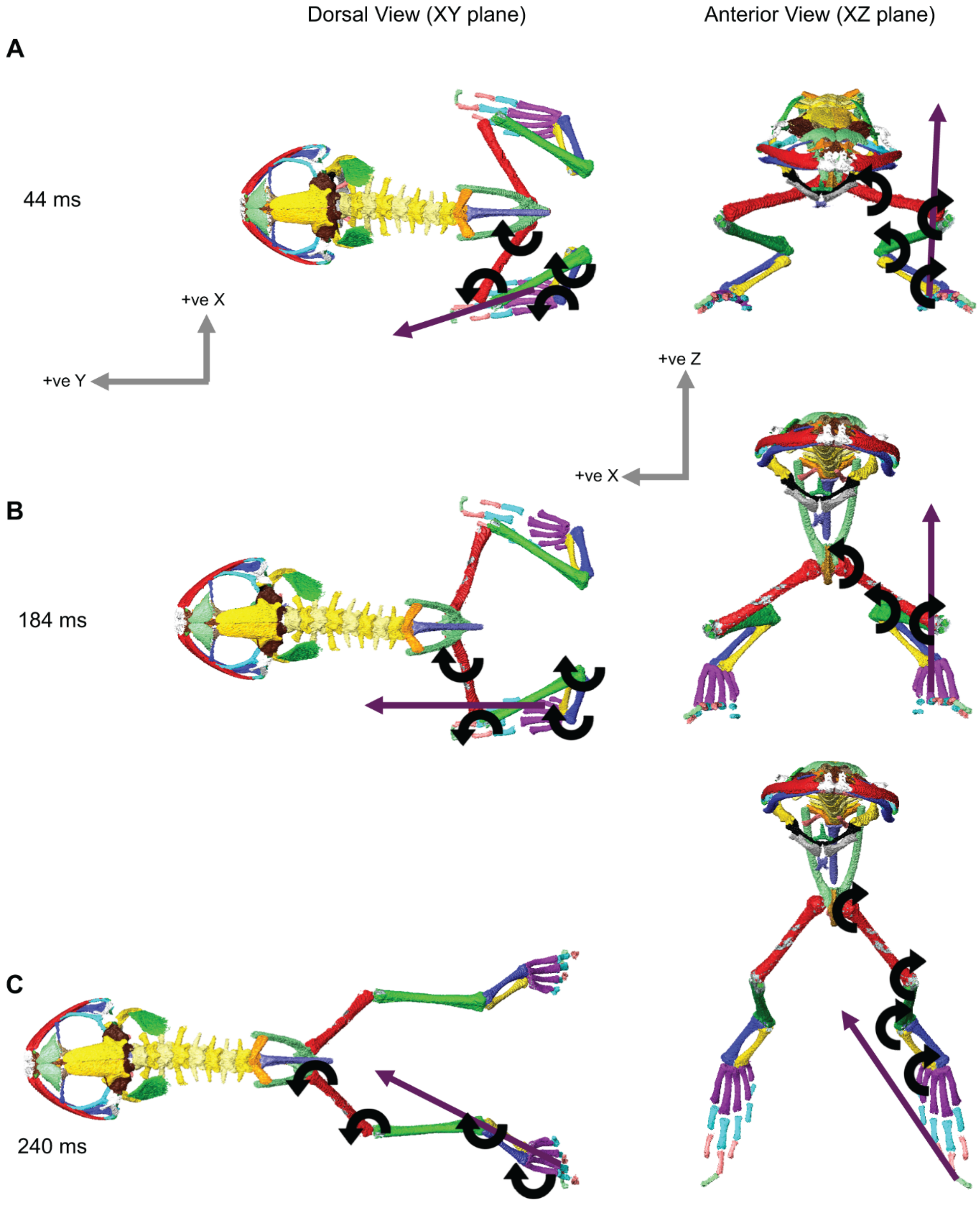

Fig. 6. External torques about the hind limb joints of *Kassina maculata* during jumping. 3D skeletal models of *K. maculata* in dorsal (A-C) and anterior (D-F) views, with global coordinates shown; forelimbs are not included in the models. Postures are based on external kinematic data from KM04 HOP 09. Models show the frog early in the jump (A,D), in mid-jump (B,E) and just prior to take-off (C,F). Purple arrows shows the direction (but

not magnitude) of the GRF in XY and XZ planes. Curved black arrows show the direction of the external moment produced at the joint by the GRF.

Tables

Table 1. Mean peak force magnitudes, ratios and timings (data from a single foot unless indicated); average peak velocity and acceleration, and timings; mean jump angles and distance.

Subject #	Mean Peak DV [A] Force (N)	Mean Peak AP [A] Force (N)	Mean Peak Total Force (N)	Total Force[B]/ Body Weight	DV /AP Force Magnitude	DV / AP Force Time (ratio)	Peak Force Time (s)[C]
KM03	-0.25 ± 0.08	-0.13 ± 0.02	0.38 ± 0.11	3.04 ± 0.791	1.94 ± 0.66	0.98	-0.06
KM04	-0.24 ± 0.09	-0.16 ± 0.04	0.36 ± 0.12	2.92 ± 0.99	1.58 ± 0.55	0.93	-0.06
KM05	-0.30 ± 0.08	-0.21 ± 0. 04	0.48 ± 0.12	2.80 ± 0.73	1.47 ± 0.49	0.99	-0.05
KM06	-0.28 ± 0.07	-0.20 ± 0.03	0.45 ± 0.10	3.24 ± 0.72	1.47 ± 0.52	0.96	-0.04
All Trials	-0.27 ± 0.09	-0.17 ± 0.04	0.41 ± 0.12	3.03 ± 0.87	1.62 ± 0.59	0.96	-0.06

Subject #	Mean Peak Velocity (ms^{-1})	Mean Peak SVL s^{-1}	Mean Peak Acceleration (ms^{-2})	Peak Velocity Time (s)[C]	Peak Acceleration Time (s)[C]	Jump Angles (°)	Jump Distance (m)
KM03	1.20 ± 0.30	20.7 ± 5.2	32.6 ± 8.1	-0.02	-0.06	34 ± 24	0.14± 0.07
KM04	1.32 ± 0.34	21.9 ± 5.7	31.3 ± 11.1	-0.02	-0.06	30 ±21	0.18± 0.09
KM05	1.47 ± 0.20	24.1 ± 3.3	38.3 ± 17.1	-0.01	-0.06	36 ± 15	0.24± 0.07
KM06	1.46 ± 0.12	24.0 ± 2.0	40.7± 9.9	-0.01	-0.07	36 ±11	0.23± 0.06
All Trials	1.36 ± 0.28	22.6 ± 4.6	35.6 ± 12.1	-0.01	-0.06	34 ± 19	0.19± 0.09
Max	2.02	33.1	79.5			69	0.34
Min	0.67	11.0	15.7			0.3	0.03

[A] Dorsoventral and anteroposterior are abbreviated DV and AP, respectively.

[B] Total force scaled to body weight accounts for forces from both hind limbs.

[C] Timings assume take-off occurs at time = 0.

Journal of Experimental Biology • Advance article

Table 2. 3D joint and body angles, and angular velocities (separated by jump angle) during jumping in *Kassina maculata*.

Subject #	Mean Ankle Range (°)	Mean Max Ankle Angle (°)	Mean Knee Range (°)	Mean Max Knee Angle (°)	Mean Hip Range (°)	Mean Max Hip Angle (°)	Mean SI[A] Range (°)	Mean Max SI[A] Angle (°)	Mean Body Range (°)	Mean Max Body Angle (°)
KM03	95	144	101	129	82	132	22	165	20	35
KM04	102	146	108	146	86	152	16	158	14	31
KM05	101	148	112	143	84	140	21	168	15	31
KM06	104	153	110	142	84	136	18	165	14	31
All trials	101	148	108	140	84	140	19	163	16	32

Jump Angle	Mean Peak Ankle Joint Angular Velocity (rad/s)	Mean Peak Knee Joint Angular Velocity (rad/s)	Mean Peak Hip Joint Angular Velocity (rad/s)	Mean Peak SI[A] Joint Angular Velocity (rad/s)	Mean Peak Body Joint Angular Velocity (rad/s)
Low	36.09	29.22	23.22	9.39	5.09
Mid	50.05	40.22	27.58	10.41	6.17
High	61.47	46.75	33.47	10.07	7.78
All trials	49.39	39.05	27.98	10.06	6.31

[A] SI = Sacroiliac.

Journal of Experimental Biology • Advance article

Table 3. 3D external moment arms and external torques from inverse dynamics analyses.

Subject #	Mean Max 3D TMT Moment Arm (m)	Mean Max 3D Ankle Moment Arm (m)	Mean Max 3D Knee Moment Arm (m)	Mean Max 3D Hip Moment Arm (m)
KM03	0.017 ± 0.005	0.022 ± 0.007	0.032 ± 0.012	0.041 ± 0.019
KM04	0.016 ± 0.005	0.021 ± 0.006	0.031 ± 0.010	0.041 ± 0.018
KM05	0.018 ± 0.004	0.024 ± 0.007	0.028 ± 0.013	0.035 ± 0.018
KM06	0.017 ± 0.004	0.025 ± 0.007	0.039 ± 0.015	0.051 ± 0.020
Low Jumps	0.020 ± 0.004	0.027 ± 0.006	0.040 ± 0.009	0.053 ± 0.013
Mid. Jumps	0.017 ± 0.004	0.024 ± 0.007	0.033 ± 0.014	0.043 ± 0.020
High Jumps	0.013 ± 0.004	0.018 ± 0.006	0.026 ± 0.012	0.032 ± 0.020
All Trials	0.017 ± 0.005	0.023 ± 0.007	0.033 ± 0.013	0.043 ± 0.020

Type	TMT Ext. Torque (N.m)	Ankle Ext. Torque (N.m)	Knee Ext. Torque (N.m)	Ext. Hip Torque (N.m)
Mean Max 3D - *All*	0.003	0.004	0.003	0.004
Mean Max 3D - *Low*	0.002	0.003	0.003	0.002
Mean Max 3D - *Mid*	0.003	0.005	0.003	0.004
Mean Max 3D - *High*	0.003	0.005	0.004	0.004
Mean Max XY - *All*	0.001	0.001	0.002	0.001
Mean Max XY - *Low*	0.001	<0.001	0.002	0.001
Mean Max XY - *Mid*	0.002	0.001	0.002	0.001
Mean Max XY - *High*	0.002	0.001	0.003	0.001
Mean Min XY - *All*	-0.002	-0.004	-0.001	-0.003

Mean Min XY - *Low*	-0.002	-0.003	-0.001	-0.002
Mean Min XY - *Mid*	-0.002	-0.004	-0.001	-0.003
Mean Min XY - *High*	-0.002	-0.004	-0.001	-0.004
Mean Max XZ - *All*	0.001	0.004	0.001	0.002
Mean Max XZ - *Low*	0.001	0.002	<0.001	0.002
Mean Max XZ - *Mid*	0.001	0.004	0.001	0.003
Mean Max XZ - *High*	0.001	0.004	0.001	0.002
Mean Min XZ - *All*	-0.002	-0.001	-0.002	<-0.001
Mean Min XZ - *Low*	-0.001	-0.001	-0.002	-0.001
Mean Min XZ - *Mid*	-0.002	<-0.001	-0.002	<-0.001
Mean Min XZ - *High*	-0.002	<-0.001	-0.003	<-0.001

Table 4. Jumping performance metrics in *Kassina maculata* compared to other frog taxa for which comparable data is available.

Species	Peak GRF (single-foot force x 2 / body mass)	Peak velocity (SVL)	Max Jump Distance (SVL)	Mean Jump angle (°)	Jump angle range (°)
Bombina[1,14]	4.2	31-43	n/a	n/a	n/a
Bufo[2]	n/a	n/a	n/a	31	14 - 51
Melanophryniscus[14]	2.3	23	n/a	n/a	n/a
Phrynoidis[14]	4.9	26	n/a	n/a	n/a
Anaxyrus[14]	2.6	16	n/a	n/a	n/a
Scaphiopus[14]	3.3	30	n/a	n/a	n/a
Hylids (5 species)[3,4,14]	6.5	45 - 115	13 - 32	40	n/a
Phyllomedusa[14]	2.4	28	n/a	n/a	n/a
Litoria[14]	5.2	52	n/a	n/a	n/a
Kassina maculata	**4.9**	**33**	**6**	**34**	**0.3 - 69**
Kassina senegalensis[14]	3.8	30	n/a	n/a	n/a
Heterixalus[14]	2.7	37	n/a	n/a	n/a
Phrynomantis[14]	2.2	20	n/a	n/a	n/a
Kaloula[14]	3	20	n/a	n/a	n/a
Rana catesbeiana[3, 5,6]	n/a	15	6	42	~10 - 60

Rana dybowskii[7]	2	n/a	5	n/a	~35 - 50
Rana esculenta[8,9]	2.7	n/a	n/a	40	n/a
Rana nigromaculata[1]	n/a	53	n/a	n/a	n/a
Rana pipiens[10-12]	4.8	56	9	26	16 - 42
Rana temporaria[13]	3.6	n/a	n/a	34	n/a
Rana rugosa[1]	n/a	50	n/a	n/a	n/a
Polypedates[14]	6	46	n/a	n/a	n/a

[1]Choi and Park, 1996; [2]Gillis and Biewener, 2000; [3]Marsh, 1994; [4]Marsh and John-Alder, 1994; [5]Olson and Marsh, 1998; [6]Astley et al. 2013; [7]Wang et al. 2014; [8]Nauwelaerts and Aerts, 2003; [9]Nauwelaerts and Aerts, 2003; [10]Hirano and Rome, 1984; [11]Lutz and Rome, 1996a; [12]Astley and Roberts, 2014; [13]Calow and Alexander, 1973; [14]Astley, 201

Table S1. Experimental summary, including information on subjects and trials, and body segment properties from CT scans for KM07.

Subject #	Mass (g)	SVL (mm)	# Trials	
KM03	25.5	58	12	
KM04	25.5	60	15	
KM05	34.6	61	8	
KM06	28.1	61	15	
Segment	**Mass (g)**	**I_X (g cm^2)**	**I_Y (g cm^2)**	**I_Z (g cm^2)**
Body	7.2	33.52	4.73	33.78
Pelvis	1.3	0.72	0.34	0.7
Thigh	0.78	0.79	0.08	0.79
Shank	0.36	0.37	0.02	0.37
Tarsus	0.16	0.06	0.005	0.06
Foot	0.16	0.09	0.005	0.09

Table S2. Experimental data and results from inverse dynamics analyses during jumping in *Kassina maculata*, including: forces (single foot) exerted on the ground, kinematic performance metrics, joint and body angles (minimum, maximum and range), 3D external joint moment arm lengths, and external joint moments (torques - 3D, XY and XZ) for four individuals and 50 trials.

Trial	Peak Vertical Force (N)	Peak Fore-Aft Force (N)	Vertical/ Fore-aft Force Ratio	Peak Total Force (N)	% Body Weight of Total Force	Vertical/ Horizontal Time Ratio
KM03_HOP_01	-0.16	-0.11	1.50	0.26	1.03	1.00
KM03_HOP_02	-0.17	-0.11	1.61	0.26	1.05	0.93
KM03_HOP_03	-0.17	-0.14	1.22	0.27	1.09	0.90
KM03_HOP_04	-0.25	-0.17	1.49	0.39	1.55	0.99
KM03_HOP_05	-0.39	-0.12	3.20	0.56	2.25	1.00
KM03_HOP_06	-0.33	-0.12	2.76	0.48	1.92	1.02
KM03_HOP_07	-0.31	-0.14	2.26	0.45	1.81	1.02
KM03_HOP_08	-0.33	-0.12	2.70	0.49	1.95	1.02
KM03_HOP_09	-0.35	-0.15	2.43	0.52	2.08	1.01
KM03_HOP_10	-0.14	-0.10	1.34	0.21	0.84	0.94
KM03_HOP_11	-0.24	-0.17	1.38	0.38	1.50	0.98
KM03_HOP_12	-0.19	-0.14	1.40	0.29	1.17	0.91
KM04_HOP_01	-0.30	-0.17	1.79	0.46	1.79	0.98
KM04_HOP_02	-0.17	-0.20	0.82	0.29	1.11	0.76
KM04_HOP_03	-0.16	-0.14	1.16	0.27	1.05	1.00
KM04_HOP_04	-0.14	-0.11	1.22	0.21	0.83	0.93
KM04_HOP_05	-0.19	-0.13	1.45	0.29	1.15	0.88
KM04_HOP_06	-0.37	-0.20	1.86	0.56	2.17	0.96
KM04_HOP_07	-0.29	-0.13	2.32	0.43	1.66	1.02
KM04_HOP_08	-0.18	-0.06	2.88	0.25	1.05	0.86
KM04_HOP_09	-0.21	-0.18	1.13	0.33	1.38	0.90
KM04_HOP_10	-0.15	-0.14	1.07	0.24	0.98	0.81
KM04_HOP_11	-0.18	-0.19	0.92	0.29	1.19	0.90
KM04_HOP_12	-0.16	-0.11	1.45	0.26	1.07	1.00
KM04_HOP_13	-0.30	-0.16	1.90	0.45	1.87	0.94
KM04_HOP_14	-0.34	-0.21	1.64	0.52	2.15	1.02
KM04_HOP_15	-0.40	-0.19	2.10	0.59	2.46	1.00
KM05_HOP_01	-0.33	-0.26	1.29	0.53	1.56	0.99
KM05_HOP_02	-0.18	-0.19	0.94	0.31	0.91	0.99
KM05_HOP_03	-0.30	-0.25	1.18	0.49	1.43	1.02
KM05_HOP_04	-0.20	-0.17	1.15	0.31	0.92	0.91
KM05_HOP_05	-0.32	-0.20	1.56	0.50	1.46	0.99
KM05_HOP_06	-0.24	-0.17	1.41	0.38	1.13	0.98
KM05_HOP_07	-0.41	-0.26	1.58	0.62	1.83	1.06
KM05_HOP_08	-0.46	-0.17	2.65	0.66	1.96	0.98
KM06_HOP_01	-0.17	-0.22	0.76	0.31	1.11	0.89
KM06_HOP_02	-0.33	-0.21	1.58	0.49	1.78	0.89
KM06_HOP_03	-0.20	-0.20	0.97	0.34	1.22	0.96
KM06_HOP_04	-0.20	-0.23	0.85	0.37	1.33	0.99

Journal of Experimental Biology • Supplementary information

Table S2 (cont.)

Trial	Peak Vertical Force (N)	Peak Fore-Aft Force (N)	Vertical/ Fore-aft Force Ratio	Peak Total Force (N)	% Body Weight of Total Force	Vertical/ Horizontal Time Ratio
KM06_HOP_05	-0.16	-0.19	0.84	0.30	1.07	1.02
KM06_HOP_06	-0.32	-0.18	1.79	0.48	1.75	0.97
KM06_HOP_07	-0.19	-0.23	0.82	0.35	1.27	0.98
KM06_HOP_08	-0.22	-0.17	1.30	0.35	1.26	1.00
KM06_HOP_09	-0.30	-0.19	1.60	0.46	1.66	0.93
KM06_HOP_10	-0.35	-0.15	2.30	0.51	1.86	0.94
KM06_HOP_11	-0.34	-0.20	1.65	0.52	1.88	0.98
KM06_HOP_12	-0.41	-0.25	1.61	0.60	2.20	0.91
KM06_HOP_13	-0.36	-0.17	2.13	0.54	1.97	1.00
KM06_HOP_14	-0.38	-0.16	2.30	0.55	2.01	0.96
KM06_HOP_15	-0.35	-0.21	1.62	0.53	1.94	1.02

Journal of Experimental Biology • Supplementary information

Table S2 (cont.)

Trial	Peak Velocity (ms^{-1})	Peak Velocity (SVL)	Peak Acceleration (ms^{-2})	Angle at Take-off (°)	Jump Distance (m)
KM03_HOP_01	0.84	14.52	27.54	7.03	0.07
KM03_HOP_02	0.92	15.80	22.62	8.53	0.05
KM03_HOP_03	0.80	13.84	22.01	6.65	0.06
KM03_HOP_04	1.11	19.12	30.90	35.34	0.11
KM03_HOP_05	1.70	29.28	49.43	69.18	0.21
KM03_HOP_06	1.46	25.23	36.03	63.15	0.17
KM03_HOP_07	1.46	25.21	28.66	58.29	0.22
KM03_HOP_08	1.34	23.05	25.06	54.13	0.16
KM03_HOP_09	1.65	28.43	34.81	59.94	0.27
KM03_HOP_10	0.85	14.67	45.08	7.43	0.08
KM03_HOP_11	1.14	19.64	36.37	23.13	0.12
KM03_HOP_12	1.15	19.87	32.50	19.56	0.14
KM04_HOP_01	1.34	22.72	28.69	46.44	0.21
KM04_HOP_02	1.26	21.27	25.96	5.63	0.05
KM04_HOP_03	1.18	19.99	23.70	23.93	0.17
KM04_HOP_04	0.99	16.77	15.65	0.27	0.08
KM04_HOP_05	1.29	21.79	21.14	34.09	0.19
KM04_HOP_06	1.72	29.16	40.09	52.70	0.30
KM04_HOP_07	1.46	24.67	32.26	53.77	0.24
KM04_HOP_08	0.67	10.98	35.52	20.81	0.03
KM04_HOP_09	1.25	20.50	22.96	23.37	0.17
KM04_HOP_10	1.14	18.76	19.22	14.20	0.14
KM04_HOP_11	1.32	21.58	23.19	10.84	0.13
KM04_HOP_12	0.83	13.63	32.76	1.52	0.07
KM04_HOP_13	1.44	23.69	47.85	50.07	0.23
KM04_HOP_14	1.84	30.22	46.61	57.20	0.32
KM04_HOP_15	2.02	33.07	53.94	60.45	0.34
KM05_HOP_01	1.50	24.61	29.99	23.41	0.20
KM05_HOP_02	1.35	22.14	31.39	28.23	0.22
KM05_HOP_03	1.71	28.07	46.34	41.48	0.32
KM05_HOP_04	1.11	18.23	19.39	7.02	0.11
KM05_HOP_05	1.60	26.30	35.16	47.46	0.29
KM05_HOP_06	1.29	21.12	28.70	34.09	0.18
KM05_HOP_07	1.47	24.15	36.34	51.09	0.25
KM05_HOP_08	1.73	28.29	79.48	53.08	0.34
KM06_HOP_01	1.39	22.82	35.18	16.49	0.17
KM06_HOP_02	1.61	26.37	43.95	34.46	0.29
KM06_HOP_03	1.22	20.02	28.10	20.51	0.13
KM06_HOP_04	1.49	24.40	29.41	24.62	0.23
KM06_HOP_05	1.33	21.85	53.10	17.80	0.11
KM06_HOP_06	1.39	22.83	31.99	40.39	0.24
KM06_HOP_07	1.43	23.41	43.60	27.67	0.20
KM06_HOP_08	1.33	21.79	69.22	33.37	0.19

Journal of Experimental Biology • Supplementary information

Table S2 (cont.)

Trial	Peak Velocity (m/s)	Peak Velocity (SVL)	Peak Acceleration (m/s2)	Angle at Take-off (°)	Jump Distance (m)
KM06_HOP_09	1.45	23.83	34.71	44.31	0.25
KM06_HOP_10	1.51	24.77	42.06	47.90	0.28
KM06_HOP_11	1.61	26.42	42.04	46.40	0.31
KM06_HOP_12	1.60	26.18	42.09	44.70	0.28
KM06_HOP_13	1.40	22.88	43.74	46.43	0.23
KM06_HOP_14	1.56	25.58	34.49	51.00	0.27
KM06_HOP_15	1.64	26.81	36.89	44.48	0.31

Table S2 (cont.)

Trial	Ankle Range (°)	Ankle Min (°)	Ankle Max (°)	Knee Range (°)	Knee Min (°)	Knee Max (°)
KM03_HOP_01	77.96	47.88	125.84	87.94	34.38	122.32
KM03_HOP_02	85.37	43.51	128.88	76.69	37.64	114.33
KM03_HOP_03	81.38	50.33	131.72	90.00	31.99	121.99
KM03_HOP_04	95.64	53.05	148.69	113.51	28.30	141.81
KM03_HOP_05	111.84	42.33	154.17	126.50	29.82	156.32
KM03_HOP_06	106.19	42.95	149.14	116.95	33.92	150.87
KM03_HOP_07	115.48	35.46	150.94	122.76	32.04	154.80
KM03_HOP_08	118.04	38.80	156.85	121.94	32.48	154.43
KM03_HOP_09	91.78	57.98	149.75	88.78	23.45	112.24
KM03_HOP_10	81.77	61.04	142.81	77.44	18.49	95.93
KM03_HOP_11	83.64	59.14	142.79	94.01	18.14	112.14
KM03_HOP_12	94.68	50.70	145.39	94.17	18.76	112.93
KM04_HOP_01	114.47	48.60	163.07	125.38	37.11	162.49
KM04_HOP_02	113.04	41.68	154.71	90.00	49.99	139.99
KM04_HOP_03	116.63	38.55	155.18	94.73	59.25	153.98
KM04_HOP_04	96.05	45.06	141.11	86.45	47.65	134.09
KM04_HOP_05	112.35	46.05	158.40	108.07	40.17	148.24
KM04_HOP_06	119.51	42.04	161.54	121.73	39.93	161.66
KM04_HOP_07	114.19	44.97	159.16	117.58	36.22	153.80
KM04_HOP_08	90.99	38.60	129.59	89.99	38.55	128.54
KM04_HOP_09	108.62	31.88	140.50	111.41	35.99	147.40
KM04_HOP_10	91.21	46.92	138.14	107.50	29.28	136.78
KM04_HOP_11	94.33	43.38	137.71	103.34	34.38	137.72
KM04_HOP_12	87.86	43.74	131.59	100.27	33.99	134.26
KM04_HOP_13	91.67	49.51	141.18	123.09	27.85	150.93
KM04_HOP_14	89.09	49.97	139.06	121.13	30.02	151.16
KM04_HOP_15	93.58	50.20	143.78	120.24	32.47	152.71
KM05_HOP_01	102.56	46.56	149.11	112.30	32.99	145.30
KM05_HOP_02	105.56	42.71	148.27	113.36	29.94	143.30
KM05_HOP_03	101.90	49.51	151.42	111.77	28.63	140.40
KM05_HOP_04	97.80	40.04	137.84	92.43	31.32	123.75
KM05_HOP_05	95.64	50.38	146.02	114.37	28.49	142.86
KM05_HOP_06	101.82	40.83	142.65	113.81	26.61	140.42
KM05_HOP_07	103.38	50.89	154.27	123.57	29.31	152.88
KM05_HOP_08	100.78	51.31	152.09	116.74	38.47	155.21
KM06_HOP_01	94.52	52.70	147.22	110.65	30.00	140.65
KM06_HOP_02	111.65	45.83	157.48	114.15	33.93	148.08
KM06_HOP_03	95.49	52.35	147.84	102.57	39.82	142.39
KM06_HOP_04	97.61	56.45	154.06	114.87	30.71	145.58
KM06_HOP_05	101.47	49.03	150.50	112.66	29.49	142.14
KM06_HOP_06	109.52	43.38	152.90	113.57	33.24	146.82
KM06_HOP_07	100.99	49.04	150.03	115.09	29.00	144.09
KM06_HOP_08	100.07	53.97	154.04	88.47	51.32	139.79

Table S2 (cont.)

Trial	Ankle Range (°)	Ankle Min (°)	Ankle Max (°)	Knee Range (°)	Knee Min (°)	Knee Max (°)
KM06_HOP_09	101.48	49.98	151.46	116.45	30.14	146.58
KM06_HOP_10	110.56	45.47	156.02	111.86	27.65	139.50
KM06_HOP_11	92.82	48.41	141.24	113.31	32.96	146.27
KM06_HOP_12	107.42	46.36	153.78	105.66	27.87	133.54
KM06_HOP_13	110.43	48.82	159.25	114.03	29.92	143.96
KM06_HOP_14	115.70	41.24	156.94	118.60	25.98	144.58
KM06_HOP_15	109.87	45.07	154.94	115.88	29.53	145.41

Table S2 (cont.)

Trial	Hip Range (°)	Hip Min (°)	Hip Max (°)	Sacroiliac Range (°)	Sacroiliac Min (°)	Sacroiliac Max (°)
KM03_HOP_01	74.02	62.97	136.99	19.07	146.45	165.52
KM03_HOP_02	74.65	56.57	131.22	9.16	148.67	157.84
KM03_HOP_03	79.33	59.42	138.76	15.16	151.01	166.17
KM03_HOP_04	88.43	51.92	140.35	24.08	138.12	162.20
KM03_HOP_05	96.86	49.64	146.50	23.43	140.04	163.47
KM03_HOP_06	91.23	56.01	147.24	29.02	137.70	166.72
KM03_HOP_07	102.83	43.80	146.63	28.42	136.98	165.39
KM03_HOP_08	101.55	44.90	146.45	27.65	137.24	164.89
KM03_HOP_09	61.64	39.51	101.16	23.03	146.24	169.27
KM03_HOP_10	62.22	52.99	115.21	22.72	143.85	166.57
KM03_HOP_11	69.88	45.83	115.71	19.76	145.90	165.66
KM03_HOP_12	79.33	39.57	118.90	20.96	140.60	161.56
KM04_HOP_01	96.04	50.04	146.08	17.49	133.13	150.62
KM04_HOP_02	97.37	47.35	144.72	24.42	129.46	153.89
KM04_HOP_03	83.61	56.06	139.67	14.65	137.92	152.57
KM04_HOP_04	71.71	70.54	142.25	10.35	145.59	155.93
KM04_HOP_05	73.63	71.08	144.71	6.21	144.39	150.60
KM04_HOP_06	97.54	54.30	151.84	16.29	144.72	161.01
KM04_HOP_07	86.35	63.05	149.40	17.89	143.29	161.18
KM04_HOP_08	63.86	87.38	151.24	14.84	145.61	160.44
KM04_HOP_09	87.16	65.30	152.46	14.23	143.14	157.37
KM04_HOP_10	72.39	86.40	158.80	14.47	147.63	162.10
KM04_HOP_11	90.04	76.05	166.09	28.31	138.53	166.84
KM04_HOP_12	87.75	62.72	150.47	10.66	145.79	156.45
KM04_HOP_13	93.09	66.65	159.74	12.27	147.58	159.84
KM04_HOP_14	94.00	64.83	158.83	12.97	141.78	154.75
KM04_HOP_15	97.01	63.81	160.81	25.64	141.85	167.49
KM05_HOP_01	89.33	49.35	138.68	19.16	146.88	166.03
KM05_HOP_02	83.05	56.21	139.25	16.04	143.96	160.00
KM05_HOP_03	83.91	51.69	135.60	24.41	147.89	172.30
KM05_HOP_04	68.41	61.57	129.98	16.63	143.97	160.60
KM05_HOP_05	80.51	61.89	142.41	22.80	149.72	172.51
KM05_HOP_06	83.28	52.07	135.35	17.69	148.39	166.08
KM05_HOP_07	90.43	56.97	147.41	28.91	144.91	173.81
KM05_HOP_08	92.76	58.55	151.31	19.29	152.64	171.93
KM06_HOP_01	78.08	55.40	133.48	6.49	153.81	160.31
KM06_HOP_02	87.12	54.72	141.84	14.72	149.34	164.06
KM06_HOP_03	86.91	44.58	131.49	13.86	145.38	159.24
KM06_HOP_04	76.99	61.16	138.15	16.64	146.31	162.95
KM06_HOP_05	72.53	60.92	133.44	17.16	141.91	159.07
KM06_HOP_06	85.74	50.89	136.63	19.02	149.23	168.25
KM06_HOP_07	80.81	59.35	140.16	12.15	149.99	162.14
KM06_HOP_08	76.24	53.23	129.48	19.18	139.88	159.06

Table S2 (cont.)

Trial	Hip Range (°)	Hip Min (°)	Hip Max (°)	Sacroiliac Range (°)	Sacroiliac Min (°)	Sacroiliac Max (°)
KM06_HOP_09	85.01	56.42	141.43	24.19	142.65	166.83
KM06_HOP_10	86.04	48.59	134.63	23.10	145.75	168.85
KM06_HOP_11	87.20	49.87	137.07	15.70	153.89	169.59
KM06_HOP_12	84.27	46.11	130.39	17.11	152.34	169.45
KM06_HOP_13	91.92	46.55	138.47	24.12	146.03	170.15
KM06_HOP_14	92.31	44.88	137.19	27.68	140.45	168.13
KM06_HOP_15	97.02	39.06	136.08	17.58	148.95	166.53

Journal of Experimental Biology • Supplementary information

Table S2 (cont.)

Trial	Sacroiliac Take-off (°)	Body Range (°)	Body Min (°)	Body Max (°)	Body Take-off (°)
KM03_HOP_01	162.93	17.18	6.56	23.73	23.59
KM03_HOP_02	156.41	10.09	2.44	12.53	2.44
KM03_HOP_03	165.71	19.41	11.73	31.14	31.14
KM03_HOP_04	160.35	20.90	10.60	31.51	30.13
KM03_HOP_05	162.67	38.62	17.68	56.30	55.21
KM03_HOP_06	164.91	29.21	30.65	59.85	59.85
KM03_HOP_07	165.23	30.88	23.20	54.08	53.78
KM03_HOP_08	159.76	32.20	20.34	52.54	52.54
KM03_HOP_09	168.51	19.53	20.98	40.51	38.85
KM03_HOP_10	166.21	7.12	14.06	21.18	19.08
KM03_HOP_11	158.80	9.01	12.05	21.06	14.85
KM03_HOP_12	157.39	7.17	13.32	20.49	13.32
KM04_HOP_01	149.05	9.32	23.17	32.49	23.17
KM04_HOP_02	150.07	6.68	0.08	6.76	2.52
KM04_HOP_03	151.22	10.28	8.52	18.79	8.52
KM04_HOP_04	154.70	13.47	0.57	14.04	6.02
KM04_HOP_05	150.60	8.35	21.05	29.40	21.05
KM04_HOP_06	160.10	21.71	22.95	44.67	42.06
KM04_HOP_07	158.74	23.14	26.58	49.72	45.93
KM04_HOP_08	152.84	8.94	15.29	24.23	15.29
KM04_HOP_09	156.03	8.39	15.86	24.24	17.64
KM04_HOP_10	159.31	8.50	16.95	25.45	24.51
KM04_HOP_11	166.43	9.34	7.08	16.42	13.76
KM04_HOP_12	156.45	8.68	12.57	21.25	12.57
KM04_HOP_13	154.55	23.60	23.71	47.31	45.17
KM04_HOP_14	153.75	22.45	27.52	49.97	46.96
KM04_HOP_15	167.00	30.91	27.79	58.70	56.98
KM05_HOP_01	159.02	9.78	12.04	21.82	16.15
KM05_HOP_02	159.37	8.72	11.34	20.06	12.24
KM05_HOP_03	164.34	13.38	17.11	30.49	25.47
KM05_HOP_04	158.66	9.31	2.30	11.61	2.30
KM05_HOP_05	172.51	18.18	23.43	41.61	39.92
KM05_HOP_06	164.59	8.09	18.71	26.81	24.18
KM05_HOP_07	169.03	32.36	15.39	47.75	42.14
KM05_HOP_08	170.31	20.75	25.96	46.71	44.70
KM06_HOP_01	158.68	12.58	3.77	16.34	3.77
KM06_HOP_02	162.89	3.63	23.36	26.99	23.60
KM06_HOP_03	153.90	16.30	2.06	18.36	2.06
KM06_HOP_04	162.95	11.96	9.31	21.27	9.31
KM06_HOP_05	156.13	13.54	2.57	16.11	2.57
KM06_HOP_06	163.47	14.24	19.38	33.61	25.61
KM06_HOP_07	162.14	7.68	14.34	22.02	14.34
KM06_HOP_08	158.27	9.54	17.66	27.21	17.66

Journal of Experimental Biology • Supplementary information

Table S2 (cont.)

Trial	Sacroiliac Take-off (°)	Body Range (°)	Body Min (°)	Body Max (°)	Body Take-off (°)
KM06_HOP_09	161.50	20.86	14.95	35.81	29.29
KM06_HOP_10	164.68	17.60	24.97	42.57	37.10
KM06_HOP_11	164.48	16.69	23.09	39.78	33.02
KM06_HOP_12	165.20	13.13	24.98	38.11	33.78
KM06_HOP_13	168.47	19.91	25.44	45.35	43.75
KM06_HOP_14	165.91	19.41	25.49	44.90	43.26
KM06_HOP_15	162.52	16.52	21.36	37.87	34.34

Table S2 (cont.)

Trial	TMT Max Moment Arm (m)	Ankle Max Moment Arm (m)	Knee Max Moment Arm (m)	Hip Max Moment Arm (m)
KM03_HOP_01	0.023	0.032	0.042	0.058
KM03_HOP_02	0.019	0.027	0.044	0.060
KM03_HOP_03	0.023	0.029	0.036	0.047
KM03_HOP_04	0.012	0.013	0.019	0.014
KM03_HOP_05	0.009	0.011	0.019	0.015
KM03_HOP_06	0.015	0.024	0.046	0.063
KM03_HOP_07	0.022	0.031	0.047	0.064
KM03_HOP_08	0.013	0.016	0.015	0.020
KM03_HOP_09	0.014	0.016	0.016	0.019
KM03_HOP_10	0.021	0.029	0.041	0.055
KM03_HOP_11	0.019	0.021	0.033	0.037
KM03_HOP_12	0.014	0.014	0.032	0.034
KM04_HOP_01	0.018	0.023	0.025	0.032
KM04_HOP_02	0.024	0.033	0.050	0.071
KM04_HOP_03	0.021	0.029	0.043	0.058
KM04_HOP_04	0.018	0.021	0.032	0.044
KM04_HOP_05	0.015	0.017	0.018	0.023
KM04_HOP_06	0.014	0.017	0.018	0.023
KM04_HOP_07	0.012	0.014	0.034	0.047
KM04_HOP_08	0.013	0.021	0.035	0.054
KM04_HOP_09	0.022	0.026	0.041	0.059
KM04_HOP_10	0.014	0.018	0.026	0.038
KM04_HOP_11	0.015	0.023	0.043	0.062
KM04_HOP_12	0.023	0.031	0.037	0.050
KM04_HOP_13	0.011	0.016	0.019	0.020
KM04_HOP_14	0.008	0.013	0.018	0.012
KM04_HOP_15	0.007	0.012	0.019	0.016
KM05_HOP_01	0.015	0.017	0.025	0.027
KM05_HOP_02	0.024	0.037	0.058	0.074
KM05_HOP_03	0.016	0.019	0.019	0.021
KM05_HOP_04	0.022	0.028	0.026	0.033
KM05_HOP_05	0.016	0.021	0.019	0.026
KM05_HOP_06	0.023	0.032	0.040	0.052
KM05_HOP_07	0.018	0.022	0.022	0.030
KM05_HOP_08	0.014	0.017	0.017	0.015
KM06_HOP_01	0.022	0.031	0.054	0.069
KM06_HOP_02	0.018	0.028	0.052	0.067
KM06_HOP_03	0.021	0.031	0.052	0.067
KM06_HOP_04	0.022	0.032	0.048	0.062
KM06_HOP_05	0.023	0.033	0.053	0.069
KM06_HOP_06	0.022	0.032	0.051	0.066
KM06_HOP_07	0.012	0.016	0.021	0.029
KM06_HOP_08	0.016	0.027	0.050	0.068

Table S2 (cont.)

Trial	TMT Max Moment Arm (m)	Ankle Max Moment Arm (m)	Knee Max Moment Arm (m)	Hip Max Moment Arm (m)
KM06_HOP_09	0.010	0.015	0.018	0.018
KM06_HOP_10	0.012	0.015	0.016	0.020
KM06_HOP_11	0.018	0.024	0.030	0.041
KM06_HOP_12	0.011	0.017	0.016	0.022
KM06_HOP_13	0.018	0.022	0.023	0.032
KM06_HOP_14	0.018	0.029	0.049	0.065
KM06_HOP_15	0.020	0.031	0.050	0.066

Table S2 (cont.)

Trial	TMT 3D Max Torque (N.m)	Ankle 3D Max Torque (N.m)	Knee 3D Max Torque (N.m)	Hip 3D Max Torque (N.m)	TMT XY Max Torque (N.m)	Ankle XY Max Torque (N.m)
KM03_HOP_01	0.001906	0.002583	0.003091	0.001072	0.001781	0.001218
KM03_HOP_02	0.001578	0.002139	0.003083	0.001159	0.001454	0.001353
KM03_HOP_03	0.002008	0.002813	0.003204	0.001625	0.001494	-0.0002
KM03_HOP_04	0.002673	0.003489	0.003622	0.001641	0.001751	0.002016
KM03_HOP_05	0.001693	0.003172	0.004581	0.004374	0.001484	0.002815
KM03_HOP_06	0.002157	0.002662	0.003491	0.003134	0.001378	0.001433
KM03_HOP_07	0.002687	0.003603	0.002306	0.002945	0.001553	0.000937
KM03_HOP_08	0.002618	0.003861	0.002827	0.002903	0.001483	-0.00028
KM03_HOP_09	0.002817	0.003595	0.004216	0.004005	0.001662	0.000811
KM03_HOP_10	0.001188	0.001448	0.00266	0.000887	0.00084	-7.4E-05
KM03_HOP_11	0.002492	0.003191	0.003855	0.00232	0.000791	0.000176
KM03_HOP_12	0.002193	0.002638	0.002867	0.00231	0.000745	8.76E-05
KM04_HOP_01	0.00238	0.004437	0.00223	0.00395	0.000831	0.001099
KM04_HOP_02	0.001975	0.003164	0.002753	0.00409	0.000911	6.61E-05
KM04_HOP_03	0.001845	0.002919	0.001334	0.003714	0.000863	0.001681
KM04_HOP_04	0.001646	0.002531	0.001545	0.001701	0.000738	0.001083
KM04_HOP_05	0.002128	0.003592	0.002448	0.003509	0.001436	0.000986
KM04_HOP_06	0.003725	0.006454	0.003222	0.006653	0.002279	0.000466
KM04_HOP_07	0.002396	0.004336	0.002309	0.004025	0.001153	0.000688
KM04_HOP_08	0.000882	0.001352	0.003097	0.002015	0.000599	0.000129
KM04_HOP_09	0.003293	0.005505	0.002419	0.002289	0.000556	0.001201
KM04_HOP_10	0.002302	0.003201	0.002822	0.001788	0.001485	-4.2E-05
KM04_HOP_11	0.003029	0.004888	0.002696	0.002091	0.00152	0.000615
KM04_HOP_12	0.001383	0.002727	0.002014	0.001489	0.000724	0.000552
KM04_HOP_13	0.003218	0.005288	0.00416	0.002802	0.000668	-0.00016
KM04_HOP_14	0.002415	0.004892	0.003474	0.002814	0.00116	0.000604
KM04_HOP_15	0.002495	0.004848	0.005182	0.003034	0.001236	-9.9E-05
KM05_HOP_01	0.003697	0.006155	0.003563	0.004381	0.003319	0.002403
KM05_HOP_02	0.002425	0.003686	0.001363	0.003105	0.001701	-0.00031
KM05_HOP_03	0.004916	0.007434	0.002401	0.005855	0.00387	0.000399
KM05_HOP_04	0.003109	0.004889	0.002852	0.002733	0.0014	-0.00011
KM05_HOP_05	0.004283	0.006756	0.002608	0.005888	0.001907	-0.00015
KM05_HOP_06	0.00291	0.005075	0.002707	0.00302	0.001191	-0.00057
KM05_HOP_07	0.004527	0.007932	0.004611	0.005534	0.002102	-0.00083
KM05_HOP_08	0.003605	0.00625	0.005082	0.007273	0.00292	0.003491
KM06_HOP_01	0.003181	0.005276	0.00228	0.005791	0.001019	0.000354
KM06_HOP_02	0.003739	0.005996	0.003195	0.006111	0.001202	0.001185
KM06_HOP_03	0.002187	0.00384	0.001328	0.003321	0.001005	0.001128
KM06_HOP_04	0.002439	0.004969	0.002666	0.006414	0.001092	0.000448
KM06_HOP_05	0.002452	0.004111	0.001427	0.004295	0.000988	0.000484
KM06_HOP_06	0.002456	0.004841	0.002471	0.004694	0.002142	0.002165
KM06_HOP_07	0.0024	0.004553	0.001613	0.004519	0.001292	0.000564

Table S2 (cont.)

Trial	TMT 3D Max Torque (N.m)	Ankle 3D Max Torque (N.m)	Knee 3D Max Torque (N.m)	Hip 3D Max Torque (N.m)	TMT XY Max Torque (N.m)	Ankle XY Max Torque (N.m)
KM06_HOP_08	0.002853	0.00462	0.001539	0.004994	0.001773	0.000852
KM06_HOP_09	0.002712	0.004743	0.003048	0.003336	0.001911	-0.00017
KM06_HOP_10	0.002391	0.004526	0.003933	0.004756	0.001794	0.001058
KM06_HOP_11	0.003051	0.005762	0.002293	0.00666	0.002144	0.003973
KM06_HOP_12	0.00331	0.006827	0.00435	0.006057	0.00194	0.000499
KM06_HOP_13	0.003341	0.005878	0.002477	0.004506	0.001805	-0.00078
KM06_HOP_14	0.0028	0.005683	0.002807	0.005751	0.001674	0.000828
KM06_HOP_15	0.00263	0.005778	0.002371	0.005911	0.001429	0.001008

Table S2 (cont.)

Trial	Knee XY Max Torque (N.m)	Hip XY Max Torque (N.m)	TMT XY Min Torque (N.m)	Ankle XY Min Torque (N.m)	Knee XY Min Torque (N.m)	Hip XY Min Torque (N.m)
KM03_HOP_01	0.002546	0.000779	-0.00065	-0.00232	-0.0011	-0.00071
KM03_HOP_02	0.002573	0.000668	-0.0005	-0.00176	0.000295	-0.00094
KM03_HOP_03	0.002276	0.001247	-0.0018	-0.00264	0.000258	-0.00062
KM03_HOP_04	0.003022	0.000924	-0.00174	-0.00306	0.000193	-0.00139
KM03_HOP_05	0.002794	0.001493	-0.00083	-0.00098	-0.00303	-0.00386
KM03_HOP_06	0.003232	0.002002	-0.00069	-0.00236	-0.00216	-0.00282
KM03_HOP_07	0.00202	-0.00045	-0.00174	-0.00314	-0.00141	-0.00256
KM03_HOP_08	0.002617	0.000206	-0.00157	-0.00349	-0.00015	-0.00265
KM03_HOP_09	0.003702	0.001091	-0.00181	-0.00327	-0.00176	-0.00346
KM03_HOP_10	0.002136	0.000487	-0.00095	-0.00135	0.000193	-0.00055
KM03_HOP_11	0.003231	0.000826	-0.00213	-0.00294	-0.00127	-0.00189
KM03_HOP_12	0.002593	0.000376	-0.00185	-0.00236	-0.00186	-0.00188
KM04_HOP_01	0.002	0.000855	-0.00203	-0.00398	-0.00137	-0.00343
KM04_HOP_02	0.002062	0.000876	-0.00162	-0.00286	0.000202	-0.00295
KM04_HOP_03	0.000614	0.000438	-0.00139	-0.0027	-0.00108	-0.00301
KM04_HOP_04	0.001358	0.00067	-0.00147	-0.00242	-0.00106	-0.00138
KM04_HOP_05	0.001762	0.000601	-0.00164	-0.00339	-0.00138	-0.0028
KM04_HOP_06	0.00233	0.000801	-0.00204	-0.00592	-0.00102	-0.00558
KM04_HOP_07	0.002002	0.001146	-0.00184	-0.00392	-0.00149	-0.00346
KM04_HOP_08	0.002933	0.001894	-0.00078	-0.00126	0.000263	-0.00149
KM04_HOP_09	0.002009	0.000488	-0.003	-0.00487	-0.00104	-0.00182
KM04_HOP_10	0.002586	0.001319	-0.00196	-0.00292	-0.00014	-0.00117
KM04_HOP_11	0.00242	0.001063	-0.00257	-0.00433	-0.00179	-0.0017
KM04_HOP_12	0.001677	0.000502	-0.00121	-0.00237	-0.00097	-0.00116
KM04_HOP_13	0.003639	0.001083	-0.00283	-0.0047	0.000465	-0.00231
KM04_HOP_14	0.002971	0.001013	-0.00153	-0.00435	-0.00154	-0.00197
KM04_HOP_15	0.004641	0.001127	-0.00158	-0.0043	0.000658	-0.0026
KM05_HOP_01	0.002986	0.000471	-0.00041	-0.00562	-0.00178	-0.00344
KM05_HOP_02	0.001044	0.000325	0.000222	-0.00334	-0.00072	-0.00232
KM05_HOP_03	0.002146	0.000907	-0.00216	-0.00676	-0.00142	-0.00461
KM05_HOP_04	0.002452	-1.7E-05	-0.00286	-0.00448	0.000239	-0.00216
KM05_HOP_05	0.002422	0.000832	-0.00333	-0.00623	-0.00036	-0.00468
KM05_HOP_06	0.002383	0.000297	-0.00255	-0.00451	-0.00036	-0.00225
KM05_HOP_07	0.003531	0.000684	-0.00372	-0.00711	-0.0007	-0.0045
KM05_HOP_08	0.000163	0.001621	-0.0004	-0.00546	-0.00454	-0.00626
KM06_HOP_01	0.00077	0.000546	-0.00265	-0.00449	-0.00172	-0.00415
KM06_HOP_02	0.000305	0.00027	-0.00307	-0.00549	-0.0027	-0.00504
KM06_HOP_03	0.000493	0.000829	-0.0017	-0.00348	-0.00099	-0.00258
KM06_HOP_04	-0.00072	0.001419	-0.00222	-0.00424	-0.00245	-0.00414
KM06_HOP_05	0.000915	0.000828	-0.00208	-0.00354	-0.00131	-0.00285
KM06_HOP_06	-0.00023	-0.00049	-0.00071	-0.00445	-0.00202	-0.00408
KM06_HOP_07	0.00128	0.00052	-0.00198	-0.00397	-0.00137	-0.00308

Table S2 (cont.)

Trial	Knee XY Max Torque (N.m)	Hip XY Max Torque (N.m)	TMT XY Min Torque (N.m)	Ankle XY Min Torque (N.m)	Knee XY Min Torque (N.m)	Hip XY Min Torque (N.m)
KM06_HOP_08	0.000592	0.001413	-0.00211	-0.00425	-0.00142	-0.00395
KM06_HOP_09	0.002608	0.00062	-0.00147	-0.00435	-0.00055	-0.00274
KM06_HOP_10	0.002671	0.002164	-0.00123	-0.00415	-0.00323	-0.00402
KM06_HOP_11	0.00066	0.001378	-0.00177	-0.00474	-0.00188	-0.00576
KM06_HOP_12	0.0036	0.000892	-0.00259	-0.00618	-0.00101	-0.0049
KM06_HOP_13	0.002197	-0.00092	-0.00242	-0.00537	-0.00088	-0.00404
KM06_HOP_14	0.002279	-0.00066	-0.0019	-0.00516	-0.00126	-0.00509
KM06_HOP_15	-0.00047	0.00101	-0.00181	-0.00531	-0.00199	-0.00505

Table S2 (cont.)

Trial	TMT XZ Max Torque (N.m)	Ankle XZ Max Torque (N.m)	Knee XZ Max Torque (N.m)	Hip XZ Max Torque (N.m)	TMT XZ Min Torque (N.m)	Ankle XZ Min Torque (N.m)
KM03_HOP_01	-4.1E-05	4.77E-05	-0.00016	0.000434	-0.00155	-0.0023
KM03_HOP_02	-3.1E-05	-0.00013	-0.00033	0.000671	-0.00123	-0.00189
KM03_HOP_03	-8.1E-05	0.000251	-5E-05	0.000546	-0.00183	-0.00263
KM03_HOP_04	-0.00011	0.000505	-0.00019	0.000924	-0.00223	-0.00321
KM03_HOP_05	-9.2E-05	0.002318	0.001534	0.001735	-0.0008	-0.00135
KM03_HOP_06	-4.7E-05	0.002355	0.001847	0.00106	-0.00152	0.000227
KM03_HOP_07	-4.8E-05	0.003168	0.001315	0.001783	-0.00223	0.000384
KM03_HOP_08	-9.4E-05	0.003255	-0.00011	0.001409	-0.00214	-0.00133
KM03_HOP_09	-8.8E-05	0.002081	0.002244	0.002295	-0.00213	-0.00142
KM03_HOP_10	3.1E-05	0.000564	0.000148	0.000559	-0.00104	-0.00137
KM03_HOP_11	-5.8E-05	0.00193	0.000131	0.001489	-0.00208	-0.00277
KM03_HOP_12	-4.8E-05	0.002192	0.000117	0.001511	-0.00193	-0.00162
KM04_HOP_01	0.00123	0.003772	-0.00031	0.001892	-0.00122	-0.00074
KM04_HOP_02	-4.2E-05	0.002402	-4.7E-05	0.00356	-0.00163	-0.00183
KM04_HOP_03	0.000692	0.002692	0.001178	0.002167	-0.0009	-0.00049
KM04_HOP_04	0.000769	0.002365	-0.00018	0.00111	-0.00142	-0.00099
KM04_HOP_05	0.001924	0.003245	-0.00022	0.002025	-0.00074	-0.00015
KM04_HOP_06	0.002651	0.005685	0.000171	0.003597	-0.00107	-0.0006
KM04_HOP_07	0.001994	0.003542	0.000267	0.001672	-0.00083	0.000247
KM04_HOP_08	-1.1E-05	0.001221	-9.5E-05	0.0019	-0.00076	-0.00092
KM04_HOP_09	0.001239	0.005023	-0.00036	0.001849	-0.0025	-0.00035
KM04_HOP_10	0.002033	0.002969	0.000127	0.001328	-0.00114	-6.8E-05
KM04_HOP_11	0.002665	0.004401	-0.00018	0.00167	-0.00115	-0.00012
KM04_HOP_12	-1.5E-05	0.002451	0.000453	0.000724	-0.00128	-0.00027
KM04_HOP_13	-3.6E-05	0.004627	-0.00034	0.001259	-0.00289	-0.00015
KM04_HOP_14	0.000219	0.004115	-0.00041	0.0015	-0.00113	0.000222
KM04_HOP_15	0.001116	0.003994	-0.00031	0.002321	-0.00152	-8.5E-05
KM05_HOP_01	-0.00017	0.005502	-0.00031	0.002989	-0.00327	-0.0017
KM05_HOP_02	-9.2E-05	0.003368	-0.00046	0.002181	-0.00221	-0.00116
KM05_HOP_03	-9.8E-05	0.006686	1.11E-05	0.004093	-0.00453	-0.00025
KM05_HOP_04	-0.00013	0.00456	-0.00025	0.002338	-0.00295	-0.0009
KM05_HOP_05	0.003397	0.006017	0.000353	0.003414	-0.0011	-0.00064
KM05_HOP_06	-9.4E-05	0.00463	-0.00038	0.002079	-0.00272	-0.00054
KM05_HOP_07	0.001828	0.006695	-0.0004	0.003203	-0.00291	-0.0028
KM05_HOP_08	-6.5E-05	0.005545	0.003471	0.002391	-0.00319	0.000124
KM06_HOP_01	0.00275	0.004461	0.001816	0.004509	-0.00045	0.000142
KM06_HOP_02	0.003176	0.004996	0.001612	0.003964	-0.00041	0.000322
KM06_HOP_03	0.00147	0.003521	0.000987	0.002451	-0.00123	-0.00021
KM06_HOP_04	0.00227	0.00392	0.001926	0.004389	-0.00037	9.26E-05
KM06_HOP_05	0.002181	0.003499	0.000916	0.003134	-0.00029	0.000185
KM06_HOP_06	-0.0003	0.004349	0.002097	0.002491	-0.00222	5E-05
KM06_HOP_07	0.002186	0.003864	0.000619	0.003296	-0.00078	0.000124

Table S2 (cont.)

Trial	TMT XZ Max Torque (N.m)	Ankle XZ Max Torque (N.m)	Knee XZ Max Torque (N.m)	Hip XZ Max Torque (N.m)	TMT XZ Min Torque (N.m)	Ankle XZ Min Torque (N.m)
KM06_HOP_08	0.002205	0.004161	0.001105	0.003289	-0.00152	-0.00033
KM06_HOP_09	0.001809	0.004141	0.000415	0.001933	-0.00158	-0.00022
KM06_HOP_10	0.001225	0.00388	0.002409	0.001754	-0.00166	0.000346
KM06_HOP_11	0.002136	0.00518	0.001985	0.003535	-0.00199	0.000124
KM06_HOP_12	0.002916	0.00583	0.000644	0.003827	-0.001	0.000407
KM06_HOP_13	0.00205	0.005225	0.000689	0.00291	-0.00214	0.000746
KM06_HOP_14	0.002081	0.00465	0.000898	0.002647	-0.00113	0.000472
KM06_HOP_15	0.001802	0.005065	0.000988	0.003747	-0.00135	0.000539

Table S2 (cont.)

Trial	Knee XZ Min Torque (N.m)	Hip XZ Min Torque (N.m)
KM03_HOP_01	-0.00229	-0.00058
KM03_HOP_02	-0.00242	-0.00079
KM03_HOP_03	-0.0023	-0.00099
KM03_HOP_04	-0.00297	-0.00042
KM03_HOP_05	-0.0041	-0.0015
KM03_HOP_06	-0.00309	0.000101
KM03_HOP_07	-0.00181	0.000205
KM03_HOP_08	-0.00245	9.18E-05
KM03_HOP_09	-0.00019	0.000126
KM03_HOP_10	-0.00213	-0.00022
KM03_HOP_11	-0.00332	-0.00121
KM03_HOP_12	-0.00261	-0.00034
KM04_HOP_01	-0.00183	-0.00047
KM04_HOP_02	-0.00229	-0.00079
KM04_HOP_03	-0.00052	-0.00052
KM04_HOP_04	-0.00122	-0.00077
KM04_HOP_05	-0.00188	-3E-05
KM04_HOP_06	-0.00262	-3.46E-06
KM04_HOP_07	-0.00177	0.000143
KM04_HOP_08	-0.00243	-0.00066
KM04_HOP_09	-0.00171	-0.00057
KM04_HOP_10	-0.00209	-0.00082
KM04_HOP_11	-0.00206	-0.00118
KM04_HOP_12	-0.00159	-0.00056
KM04_HOP_13	-0.00339	-0.00115
KM04_HOP_14	-0.00269	0.0002
KM04_HOP_15	-0.00419	0.000508
KM05_HOP_01	-0.00275	-0.00044
KM05_HOP_02	-0.00098	-0.00052
KM05_HOP_03	-0.00208	0.000337
KM05_HOP_04	-0.00222	-0.00026
KM05_HOP_05	-0.00217	0.000202
KM05_HOP_06	-0.00205	-0.00066
KM05_HOP_07	-0.00291	-0.00068
KM05_HOP_08	-0.00305	-0.00019
KM06_HOP_01	-0.00113	0.000106
KM06_HOP_02	-0.00234	1E-05
KM06_HOP_03	-0.0006	-0.00054
KM06_HOP_04	-0.00241	0.000949
KM06_HOP_05	-0.00127	0.000437
KM06_HOP_06	-0.00136	-3.4E-05
KM06_HOP_07	-0.00134	0.000343

Table S2 (cont.)

Trial	Knee XZ Min Torque (N.m)	Hip XZ Min Torque (N.m)
KM06_HOP_08	-0.00143	9.05E-05
KM06_HOP_09	-0.00217	-0.00053
KM06_HOP_10	-0.00343	0.000271
KM06_HOP_11	-0.0013	0.000292
KM06_HOP_12	-0.00315	0.000178
KM06_HOP_13	-0.00212	0.000268
KM06_HOP_14	-0.00216	0.000199
KM06_HOP_15	-0.00165	0.00019

Table S3. ANCOVA testing for relationship between jump angle (continuous dependent variable) due to individual (nominal covariate) and the following continuous covariates: forces exerted (dorsoventral, anteroposterior, total [scaled to body weight]); kinematic performance metrics; 3D joint/body angles (range and maximum); maximum 3D external moment arms; maximum 3D external moments; and maximum and minimum XY and XZ moments. Interaction effects between individuals and continuous covariates also shown (significant results indicate differential response to continuous covariate as a function of individual). Bold entries indicate significant results.

DV Force (N)	**df**	**SS**	**MS**	**F**	**P (sig)**
Individual	3	287.696	95.8988	1.80488	0.160972
DV Force	1	13356.8	13356.8	**251.384**	**$2.46*10^{-19}$**
Individual*DV Force	3	1547.19	515.73	**9.70638**	**0.00005**
Error	42	2231.59	53.1331		
Total	49	17423.3			

AP Force (N)	**df**	**SS**	**MS**	**F**	**P (sig)**
Individual	3	287.696	95.8988	0.25904	0.854464
AP Force	1	484.968	484.968	1.30998	0.258878
Individual*AP Force	3	1101.86	367.287	0.992108	0.405822
Error	42	15548.8	370.209		
Total	49	17423.3			

Total Force (x body weight)	**df**	**SS**	**MS**	**F**	**P (sig)**
Individual	3	287.696	95.8988	1.53137	0.220393
Total Force	1	13881.9	13881.9	**221.674**	**$2.34*10^{-18}$**
Individual*Tot. Force	3	623.544	207.848	**3.31904**	**0.0287781**
Error	42	2630.17	62.623		
Total	49	17423.3			

Velocity (ms^{-1})	**df**	**SS**	**MS**	**F**	**P (sig)**
Individual	3	287.696	95.8988	0.843156	0.478002
Velocity	1	11829.5	11829.5	**104.007**	**$6.22*10^{-13}$**
Individual*Velocity	3	529.067	176.356	1.55054	0.2156
Error	42	4776.99	113.738		
Total	49	17423.3			

Velocity (SVL)	**df**	**SS**	**MS**	**F**	**P (sig)**
Individual	3	287.696	95.8988	0.851031	0.473924
Velocity	1	11969.7	11969.7	**106.222**	**$4.52*10^{-13}$**
Individual*Velocity	3	433.132	144.377	1.28124	0.293219
Error	42	4732.79	112.685		
Total	49	17423.3			

Acceleration (ms^{-2})	**df**	**SS**	**MS**	**F**	**P (sig)**
Individual	3	287.696	95.8988	0.336934	0.798692
Acceleration	1	3450.38	3450.38	**12.1227**	**0.001176**
Individual*Acc.	3	1731.07	577.022	2.02733	0.124634
Error	42	11954.1	284.622		
Total	49	17423.3			

Ankle Range (°)	**df**	**SS**	**MS**	**F**	**P (sig)**
Individual	3	287.696	95.8988	0.363183	0.779897
Ankle range	1	4651.27	4651.27	**17.615**	**0.000137**
Individual*Ankle rg.	3	1394.17	464.723	1.75997	0.169504
Error	42	11090.2	264.051		
Total	49	17423.3			

Ankle Max (°)	**df**	**SS**	**MS**	**F**	**P (sig)**
Individual	3	287.696	95.8988	0.407099	0.748682
Ankle max	1	5902.35	5902.35	**25.056**	**0.000010**
Individual*Ankle mx.	3	1339.46	446.486	1.89537	0.145058
Error	42	9893.78	235.566		
Total	49	17423.3			

Knee Range (°)	**df**	**SS**	**MS**	**F**	**P (sig)**
Individual	3	287.696	95.8988	0.631812	0.598606
Knee range	1	10110.9	10110.9	**66.6135**	**$3.33*10^{-10}$**
Individual*Knee rg.	3	649.813	216.604	1.42706	0.248339
Error	42	6374.92	151.784		
Total	49	17423.3			

Knee Max (°)	**df**	**SS**	**MS**	**F**	**P (sig)**
Individual	3	287.696	95.8988	0.507499	0.679244
Knee max	1	8316.78	8316.78	**44.0126**	**$4.86*10^{-8}$**
Individual*Knee mx.	3	882.33	294.11	1.55644	0.214149
Error	42	7936.48	188.964		
Total	49	17423.3			

Hip Range (°)	**df**	**SS**	**MS**	**F**	**P (sig)**
Individual	3	287.696	95.8988	0.353913	0.786527
Hip range	1	5618.62	5618.62	**20.7354**	**0.000045**
Individual*Hip rg.	3	136.334	45.4447	0.167713	0.917563
Error	42	11380.6	270.967		
Total	49	17423.3			

Journal of Experimental Biology • Supplementary information

Hip Max (°)	**df**	**SS**	**MS**	**F**	**P (sig)**
Individual	3	287.696	95.8988	0.274202	0.84366
Hip max	1	1856.73	1856.73	**5.30891**	**0.026232**
Individual*Hip mx.	3	589.881	196.627	0.562213	0.642935
Error	42	14689	349.738		
Total	49	17423.3			

SI Range (°)	**df**	**SS**	**MS**	**F**	**P (sig)**
Individual	3	287.696	95.8988	0.35203	0.787874
SI range	1	3624.95	3624.95	**13.3066**	**0.000724**
Individual*SI rg.	3	2069.14	689.713	2.53183	0.069922
Error	42	11441.5	272.417		
Total	49	17423.3			

SI Max (°)	**df**	**SS**	**MS**	**F**	**P (sig)**
Individual	3	287.696	95.8988	0.299536	0.825526
SI max	1	2802.64	2802.64	**8.75392**	**0.005057**
Individual*SI mx.	3	886.305	295.435	0.922778	0.438132
Error	42	13446.6	320.158		
Total	49	17423.3			

Body Range (°)	**df**	**SS**	**MS**	**F**	**P (sig)**
Individual	3	287.696	95.8988	0.572218	0.63643
Body range	1	9763.16	9763.16	**58.2558**	$\mathbf{1.83*10^{-9}}$
Individual*Body rg.	3	333.594	111.198	0.663507	0.579153
Error	42	7038.83	167.591		
Total	49	17423.3			

Body Max (°)	**df**	**SS**	**MS**	**F**	**P (sig)**
Individual	3	287.696	95.8988	1.74328	0.172789
SI max	1	14735	14735	**267.858**	$\mathbf{7.79*10^{-20}}$
Individual*SI mx.	3	90.0996	30.0332	0.545953	0.653597
Error	42	2310.44	55.0106		
Total	49	17423.3			

TMT Moment Arm	**df**	**SS**	**MS**	**F**	**P (sig)**
Individual	3	287.696	95.8988	0.410203	0.746491
TMT MA	1	6668.57	6668.57	**28.5245**	$\mathbf{3.50*10^{-6}}$
Individual*TMT MA	3	648.1	216.033	0.924073	0.437508
Error	42	9818.91	233.784		
Total	49	17423.3			

Ankle Moment Arm	**df**	**SS**	**MS**	**F**	**P (sig)**
Individual	3	287.696	95.8988	0.366075	0.777831
Ankle MA	1	5150.16	5150.16	**19.6507**	**0.000065**
Individual*Ank. MA	3	982.894	327.631	1.25067	0.303568
Error	42	11002.5	261.965		
Total	49	17423.3			

Knee Moment Arm	**df**	**SS**	**MS**	**F**	**P (sig)**
Individual	3	287.696	95.8988	0.338072	0.797875
Knee MA	1	3947.19	3947.19	**13.915**	**0.000567**
Individual*Knee MA	3	1274.53	424.843	1.4977	0.22906
Error	42	11913.9	283.664		
Total	49	17423.3			

Hip Moment Arm	**df**	**SS**	**MS**	**F**	**P (sig)**
Individual	3	287.696	95.8988	0.34083	0.79483
Hip MA	1	4366.88	4366.88	**15.6228**	**0.000291**
Individual*Hip MA	3	1028.85	342.949	1.22692	0.311845
Error	42	11739.9	279.52		
Total	49	17423.3			

TMT 3D Torques	**df**	**SS**	**MS**	**F**	**P (sig)**
Individual	3	287.696	95.8988	0.305253	0.821425
TMT 3D Torques	1	3406.46	3406.46	**10.843**	**0.002017**
Individual*TMT 3D	3	534.344	178.115	0.566952	0.639848
Error	42	13194.8	314.161		
Total	49	17423.3			

Ankle 3D Torques	**df**	**SS**	**MS**	**F**	**P (sig)**
Individual	3	287.696	95.8988	0.396802	0.755967
Ankle 3D Torques	1	5809.52	5809.52	**24.0381**	**0.000015**
Individual*Ankle 3D	3	1175.55	391.85	1.62137	0.198773
Error	42	10150.5	241.679		
Total	49	17423.3			

Knee 3D Torques	**df**	**SS**	**MS**	**F**	**P (sig)**
Individual	3	287.696	95.8988	0.318502	0.811917
Knee 3D Torques	1	4043.17	4043.17	**13.4283**	**0.000689**
Individual*Knee 3D	3	446.505	148.835	0.494316	0.688169
Error	42	12645.9	301.093		
Total	49	17423.3			

Journal of Experimental Biology • Supplementary information

Hip 3D Torques	**df**	**SS**	**MS**	**F**	**P (sig)**
Individual	3	287.696	95.8988	0.487611	0.692732
Hip 3D Torques	1	6380.44	6380.44	**32.4422**	**$1.09*10^{-6}$**
Individual*Hip 3D	3	2494.99	831.662	**4.22871**	**0.010627**
Error	42	8260.16	196.671		
Total	49	17423.3			

TMT XY Max	**df**	**SS**	**MS**	**F**	**P (sig)**
Individual	3	287.696	95.8988	0.305253	0.821425
TMT XY Max	1	3406.46	3406.46	**10.843**	**0.002017**
Individual*TMT +XY	3	534.344	178.115	0.566952	0.639848
Error	42	13194.8	314.161		
Total	49	17423.3			

Ankle XY Max	**df**	**SS**	**MS**	**F**	**P (sig)**
Individual	3	287.696	95.8988	0.258043	0.855173
Ankle XY Max	1	458.15	458.15	1.23278	0.273183
Individual*Ank +XY	3	1068.57	356.191	0.958432	0.421241
Error	42	15608.9	371.64		
Total	49	17423.3			

Knee XY Max	**df**	**SS**	**MS**	**F**	**P (sig)**
Individual	3	287.696	95.8988	0.258043	0.855173
Knee XY Max	1	1798.76	1798.76	**5.54583**	**0.023273**
Individual*Knee +XY	3	1714.37	571.455	1.76188	0.169133
Error	42	13622.5	324.344		
Total	49	17423.3			

Hip XY Max	**df**	**SS**	**MS**	**F**	**P (sig)**
Individual	3	287.696	95.8988	0.260115	0.8537
Hip XY Max	1	293.119	293.119	0.795051	0.377657
Individual*Hip +XY	3	1357.95	452.649	1.22776	0.311549
Error	42	15484.5	368.679		
Total	49	17423.3			

TMT XY Min	**df**	**SS**	**MS**	**F**	**P (sig)**
Individual	3	287.696	95.8988	0.241881	0.866619
TMT XY Min	1	61.3934	61.3934	0.15485	0.695934
Individual*TMT -XY	3	422.408	140.803	0.35514	0.785648
Error	42	16651.8	396.471		
Total	49	17423.3			

Journal of Experimental Biology • Supplementary information

Ankle XY Min	**df**	**SS**	**MS**	**F**	**P (sig)**
Individual	3	287.696	95.8988	0.315427	0.814124
Ankle XY Min	1	4195.55	4195.55	**13.7998**	**0.000594**
Individual*Ankle -XY	3	170.836	56.9454	0.187303	0.904451
Error	42	12769.2	304.029		
Total	49	17423.3			

Knee XY Min	**df**	**SS**	**MS**	**F**	**P (sig)**
Individual	3	287.696	95.8988	0.289779	0.832519
Knee XY Min	1	1649.9	1649.9	**4.98554**	**0.030947**
Individual*Knee -XY	3	1586.31	528.77	1.5978	0.204225
Error	42	13899.4	330.937		
Total	49	17423.3			

Hip XY Min	**df**	**SS**	**MS**	**F**	**P (sig)**
Individual	3	287.696	95.8988	0.56263	0.642663
Hip XY Min	1	8317.61	8317.61	**48.7987**	**$1.52*10^{-8}$**
Individual*Hip -XY	3	1659.19	553.063	**3.24478**	**0.031263**
Error	42	7158.79	170.447		
Total	49	17423.3			

TMT XZ Max	**df**	**SS**	**MS**	**F**	**P (sig)**
Individual	3	287.696	95.8988	0.272762	0.844688
TMT XZ Max	1	241.851	241.851	0.68789	0.411572
Individual*TMT +XZ	3	2127.21	709.07	2.01679	0.126153
Error	42	14766.5	351.584		
Total	49	17423.3			

	df	**SS**	**MS**	**F**	**P (sig)**
Ankle XZ Max					
Individual	3	287.696	95.8988	0.434353	0.729527
Ankle XZ Max	1	7366.48	7366.48	**33.3649**	**$8.33*10^{-7}$**
Individual*Ankle +XZ	3	496.114	165.371	0.749013	0.529062
Error	42	9272.99	220.786		
Total	49	17423.3			

Knee XZ Max	**df**	**SS**	**MS**	**F**	**P (sig)**
Individual	3	287.696	95.8988	0.337399	0.798358
Knee XZ Max	1	1897.94	1897.94	**6.67748**	**0.013332**
Individual*Knee +XZ	3	3300.01	1100	**3.87012**	**0.015673**
Error	42	11937.6	284.23		
Total	49	17423.3			

Hip XZ Max	**df**	**SS**	**MS**	**F**	**P (sig)**
Individual	3	287.696	95.8988	0.326399	0.80625
Hip XZ Max	1	834.745	834.745	2.84112	0.099297
Individual*Hip +XZ	3	3960.88	1320.29	**4.49372**	**0.008002**
Error	42	12340	293.809		
Total	49	17423.3			

TMT XZ Min	**df**	**SS**	**MS**	**F**	**P (sig)**
Individual	3	287.696	95.8988	0.2505	0.860525
TMT XZ Min	1	416.554	416.554	1.08809	0.302862
Individual*TMT -XZ	3	640.169	213.39	0.557401	0.646079
Error	42	16078.9	382.83		
Total	49	17423.3			

Ankle XZ Min	**df**	**SS**	**MS**	**F**	**P (sig)**
Individual	3	287.696	95.8988	0.317901	0.812349
Ankle XZ Min	1	3430.62	3430.62	**11.3724**	**0.001611**
Individual*Ankle -XZ	3	1035.14	345.048	1.14382	0.342512
Error	42	12669.8	301.662		
Total	49	17423.3			

Knee XZ Min	**df**	**SS**	**MS**	**F**	**P (sig)**
Individual	3	287.696	95.8988	0.284527	0.836279
Knee XZ Min	1	2087.35	2087.35	**6.19306**	**0.016875**
Individual*Knee -XZ	3	892.288	297.429	0.882458	0.457947
Error	42	14155.9	337.046		
Total	49	17423.3			

Hip XZ Min	**df**	**SS**	**MS**	**F**	**P (sig)**
Individual	3	287.696	95.8988	0.300264	0.825004
Hip XZ Min	1	2419.06	2419.06	**7.57421**	**0.008705**
Individual*Hip -XZ	3	1302.5	434.167	1.3594	0.268274
Error	42	13414	319.382		
Total	49	17423.3			

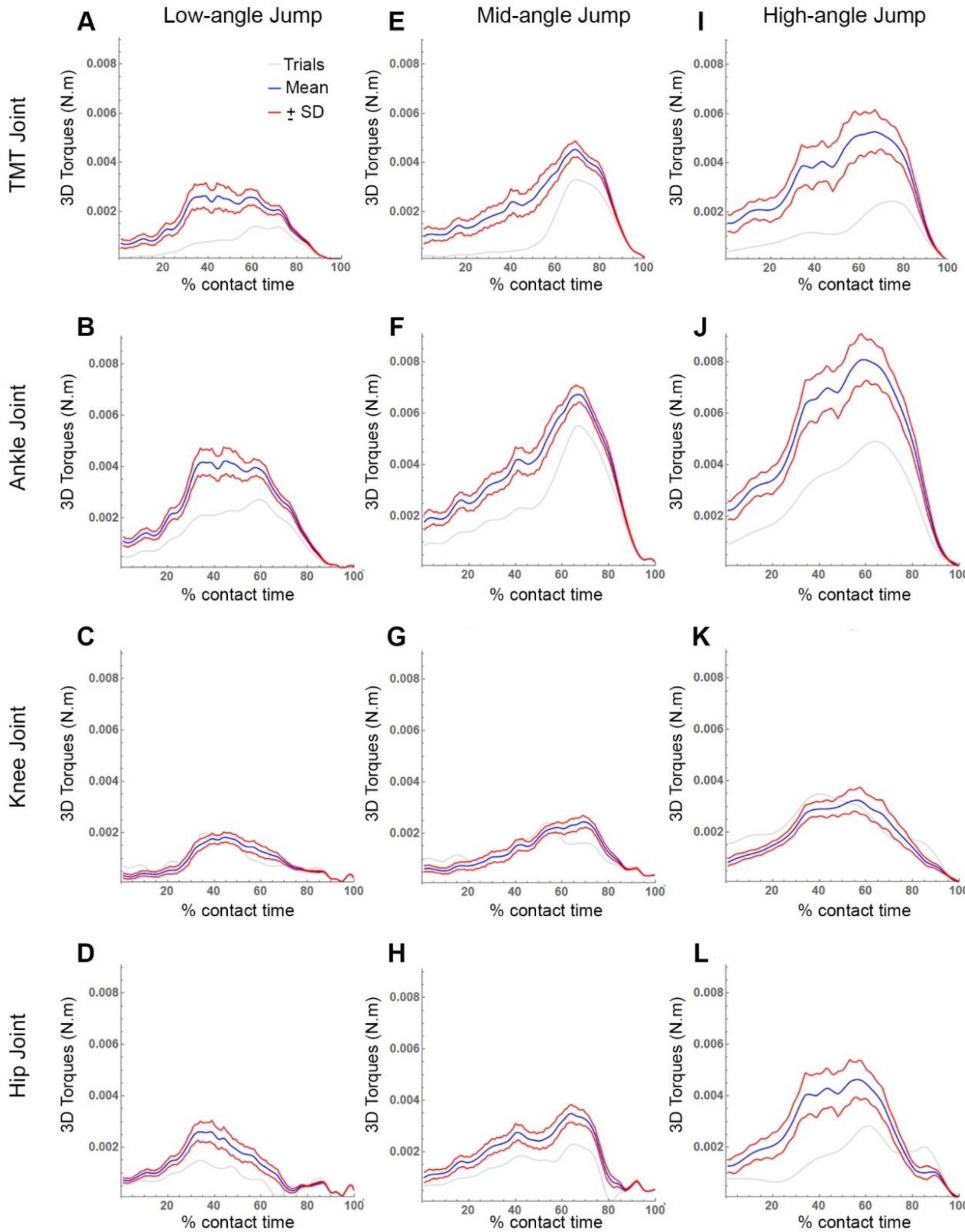

Figure S4. Sensitivity analysis of the impact of center of pressure (COP) location on three-dimensional external torques at the TMT (A, E, I), ankle (B, F, J), knee (C, G, K) and hip (D, H, L) joints during low-angle (A-D, KM04 HOP 12), intermediate (E-H, KM04 HOP 09) and high-angle (I-L, KM04 HOP 14) jumps. Data are normalized and resampled to 100 time points and are shown to the same scale. Gray trace is data from the original trial (using estimated COP as described in the text). Blue trace is the mean of 100 iterations using alternate COP locations and red traces are the standard deviations.

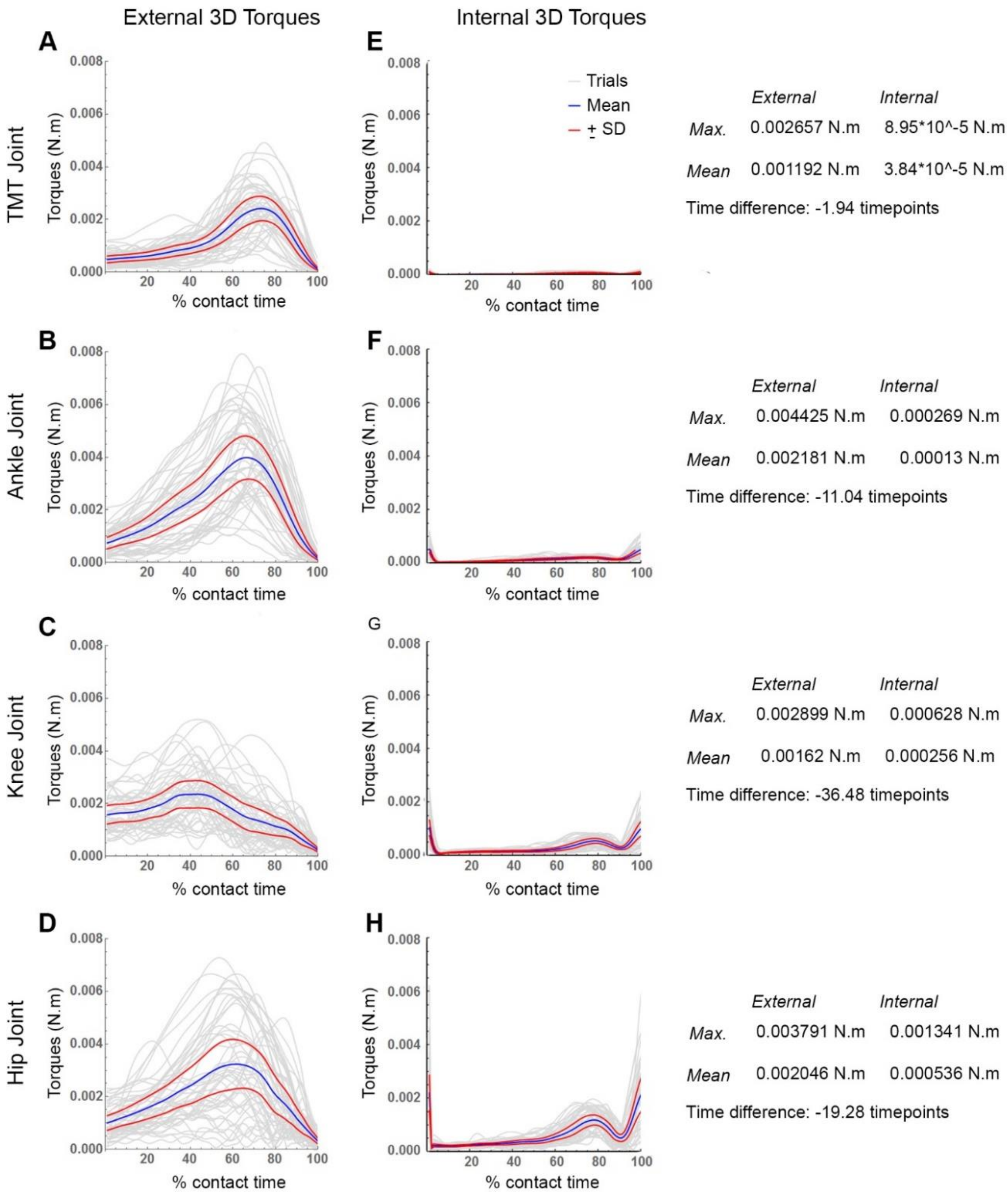

Figure S5. Comparison of 3D external (A-D) and internal (E-H) joint torques at the TMT (A, E), ankle (B, F), knee (C, G) and hip (D, H) joints for all trials. Internal torques for foot segment are negligible and not shown. Data are normalized and resampled to 100 time points and are shown to the same scale. Gray traces are data from the individual trials; blue trace is the mean and red traces are the standard deviations. Right column shows average (for all trials) peak and mean external and internal torque magnitudes, and time difference between peak values (external – internal; thus, negative values indicate external torques peaked earlier). Artefactual high internal torques during the first and last few frames should be ignored.